5-2020

Observation of Struvite in the Mixed Microalgae Biofilm Matrix of a Rotating Algal Biofilm Reactor During Nutrient Removal from Municipal Anaerobic Digester Filtrate

Kyle M. Hillman
Utah State University

OBSERVATION OF STRUVITE IN THE MIXED MICROALGAE BIOFILM MATRIX OF A ROTATING ALGAL BIOFILM REACTOR DURING NUTRIENT REMOVAL FROM MUNICIPAL ANAEROBIC DIGESTER FILTRATE

by

Kyle M. Hillman

A thesis submitted in partial fulfillment
of the requirements for the degree

of

MASTER OF SCIENCE

in

Biological Engineering

Approved:

_____	_____
Ronald C. Sims, Ph.D. Major Professor	Charles D. Miller, Ph.D. Committee Member
_____	_____
Judith L. Sims, M.S. Committee Member	Richard S. Inouye, Ph.D. Vice Provost for Graduate Studies

UTAH STATE UNIVERSITY
Logan, Utah

2020

ABSTRACT

Observation of Struvite in the Mixed Microalgae Biofilm Matrix of a Rotating Algal Biofilm Reactor During Nutrient Removal from Municipal Anaerobic Digester Filtrate

by

Kyle M. Hillman, Master of Science

Utah State University, 2020

Major Professor: Dr. Ronald C. Sims
Department: Biological Engineering

Central Valley Water Reclamation Facility (CVWRF) in Salt Lake City is the largest municipal wastewater treatment plant in Utah and must meet new and rigorous nutrient effluent standards. Filtrate from CVWRF anaerobic digesters contains high levels of nitrogen, phosphorus, and magnesium. Supersaturation of these constituents leads to nuisance struvite precipitation that clogs belts, pumps, and pipes downstream of anaerobic digesters. Struvite is a mineral precipitate with equimolar magnesium, ammonium, and phosphate. Controlled struvite precipitation helps prevent nuisance precipitation, removes phosphate, and generates a fertilizer product.

An outdoor pilot-scale rotating algal biofilm reactor (RABR) was implemented at CVWRF as a potential alternative for nitrogen and phosphorus removal from anaerobic digester (AD) filtrate. Struvite was observed within the microalgae biofilm matrix.

Despite RABR influent component ion molar ratios with potential for various

magnesium and calcium precipitates, struvite is the only phosphate precipitate observed in the microalgae biofilm. The measured average biofilm pH was 8.0, which is favorable to struvite precipitation. Struvite could potentially form in the RABR tank water at pH 7.9, but little struvite was detected in the settled sludge. Therefore, the biofilm may also provide nucleation sites that favor struvite precipitation within the biofilm.

Nitrogen and phosphorus were removed from municipal anaerobic digester pressate through biofilm growth and struvite precipitation. Microalgae biofilm can then be harvested and pelletized into fertilizer. Struvite will add fertilizer value to the product.

East vs west-facing biofilm orientation and biomass harvesting interval influence struvite content within the biofilm matrix. Three harvesting intervals were evaluated: 1-week growth (top layer), 2.5-month growth (top layer), and the bottom layer that developed over 2.5 months and served as the base layer for 1-week growth. The east bottom layer had the highest struvite content with 5% by weight of total solids. West bottom and 1-week growth contained 4.3% and 4.1% struvite, respectively. East 1-week growth and east/west 2.5-month top-layer growth ranged from 1-1.4% struvite. A higher struvite content was correlated with higher microalgae content.

This study is the first observation of biologically-enhanced struvite precipitation. A RABR system may provide an alternative technology for nutrient removal as both microalgae cultivation and struvite precipitation, which has engineering significance for wastewater treatment.

(121 pages)

PUBLIC ABSTRACT

Observation of Struvite in the Mixed Microalgae Biofilm Matrix of a Rotating Algal Biofilm Reactor During Nutrient Removal from Municipal Anaerobic Digester Filtrate

Kyle M. Hillman

Central Valley Water Reclamation Facility (CVWRF) in Salt Lake City is the largest municipal wastewater treatment plant in Utah and must meet new and rigorous nutrient effluent standards – over 95% reduction in phosphorus output by 2025. Filtrate from CVWRF anaerobic digesters contains high levels of nitrogen, phosphorus, and magnesium. Supersaturation of these constituents leads to nuisance struvite precipitation that clogs belts, pumps, and pipes downstream of anaerobic digesters. Struvite is a mineral precipitate composed of equimolar magnesium, ammonium, and phosphate. Controlled precipitation of struvite helps prevent clogging and scaling, removes phosphate from wastewater, and generates a marketable fertilizer product.

Struvite was observed within the microalgae biofilm matrix of an outdoor, pilot-scale rotating algal biofilm reactor (RABR) designed to remove nitrogen (N) and phosphorus (P) from anaerobic digester filtrate. East/west biofilm orientation and biomass harvesting interval influence struvite content within the biofilm matrix. Despite RABR influent component ion molar ratios with potential for various magnesium and calcium precipitates, microalgae biofilm provides pH, temperature, and nucleation sites favorable to struvite precipitation.

The RABR system removed N and P through biofilm growth and through struvite precipitation. Microalgae biofilm can be harvested and pelletized into fertilizer, and the struvite content will add fertilizer value to the product. More research is needed for optimization and scalability of P removal through combined microalgae biofilm and struvite precipitation.

ACKNOWLEDGMENTS

This project was made possible with funding from the Huntsman Environmental Research Center and research facilities provided by the Sustainable Waste to Bioproducts Engineering Center. Thanks to WesTech Engineering, Inc. for construction of the pilot scale rotating algal biofilm reactor, and thanks to Central Valley Water Reclamation Facility for collaboration and use of their facilities. Thank you to Dr. FenAnn Shen with the Utah State University Office of Research, Microscopy Core Institute for SEM/EDS imaging. Thank you to Dr. Philip Heck for reviewing parts of Chapter 1 that pertain to CVWRF background and side-stream P removal technologies. Thank you to Joshua Hortin with the Utah Water Research Laboratory for Mg, Ca, and P analysis via ICP-MS. Thank you to Dylan Ellis, Jacob Watkins, Steven White, and Taylor Adams for invaluable laboratory assistance and long days in the field.

None of this would have been possible without the patience and guidance of my committee members. Special thanks to Dr. Ronald Sims for guidance and mentorship every step of the way. Thank you for reminding me to “Fail Forward!” when things inevitably did not go as expected or obstacles seemed impossible to overcome.

Kyle M. Hillman

CONTENTS

Page

LIST OF TABLES

LIST OF FIGURES

ABBREVIATION KEY

AD	Anaerobic Digester
ANOVA	Analysis of Variants
Ca	Calcium
CVWRF	Central Valley Water Reclamation Facility
DI	Deionized
DWQ	Division of Water Quality
EDS	Energy Dispersive X-Ray Spectroscopy
HRT	Hydraulic Retention Time
ICP-MS	Inductively Coupled Plasma - Mass Spectroscopy
M	Molar (when referring to the molar concentration)
Mg	Magnesium
Ml	Milliliters
N	Nitrogen
N	Normal (when referring to the normality of an acid solution)
P	Phosphorus
PAR	Photosynthetically Active Radiation
RABR	Rotating Algal Biofilm Reactor
RPM	Rotations Per Minute
SEM	Scanning Electron Microscopy
SWBEC	Sustainable Waste to Bioproducts Engineering Center
TS	Total Solids
UWRL	Utah Water Research Laboratory

CHAPTER 1

OBSERVATION AND QUANTIFICATION OF STRUVITE WITHIN THE MIXED MICROALGAE BIOFILM MATRIX OF THE CENTRAL VALLEY WATER RECLAMATION FACILITY ROTATING ALGAL BIOFILM REACTOR

Introduction

Effective January 1, 2020, the Utah Division of Water Quality (DWQ) requires a Technology-Based Phosphorus Effluent Limit of 1.0 mg/L for all wastewater treatment facilities in the state. Central Valley Water Reclamation Facility (CVWRF), located in Salt Lake City, is the largest municipal wastewater treatment plant in Utah. CVWRF has been granted a five-year variance to the requirement and must meet the limit by January 1, 2025.

The facility has designed a biological nutrient removal process to remove phosphorus from the liquid stream. The sizing of this process is contingent upon implementation of an accompanying side-stream process to reduce influent nutrient loads by removing phosphorus (P) and nitrogen (N) from the plant's recycle streams. Therefore, side stream P removal was "deemed necessary" to meet the new effluent requirements [1]. Struvite precipitation is the main side-stream process that was considered for removing P at CVWRF.

Struvite forms in alkaline conditions and is normally considered a nuisance precipitate in wastewater treatment facilities because it precipitates in anaerobic digesters, biosolids pumping and piping systems, and biosolids dewatering equipment.

Struvite precipitates as a hard-mineral crystal composed of equimolar magnesium, ammonium, and phosphate.

Currently, struvite precipitation at CVWRF has been a significant issue on the belt filter press dewatering equipment downstream from the anaerobic digesters. In this process, liquid biosolids are spread onto a moving belt where the solids are retained while water is drained via gravity. After gravity drainage, the thickened solids are squeezed between two belts running in a circuitous path over rollers to remove the remaining free water.

This process releases carbon dioxide from the biosolids which raises the pH and causes struvite precipitation on the belts, rollers, drainage collection pans, and other components of the belt filter presses. In the future, with biological nutrient removal, P concentration in the digested biosolids will be significantly higher and is expected to exacerbate the scaling issues.

Side stream P removal is advantageous for two main reasons: reducing the influent load on the biological process and reducing struvite scaling. Both can be accomplished by a controlled struvite precipitation using a side stream process.

The water chemistry at CVWRF is unique, especially relative to biological phosphorus removal and struvite precipitation. Biological processes used for P removal require readily degradable carbon, but carbon is relatively low in CVWRF's influent compared to many wastewater plants. Therefore, an alternate source of carbon will be required, or the carbon requirement will need to be lowered by reducing the influent phosphorus load. Side stream removal will reduce the carbon requirement by reducing the

influent load. [1]

In addition to low readily degradable carbon levels, the wastewater at CVWRF has relatively high magnesium (Mg) and calcium (Ca) concentrations due to the geology of the local area that supplies the potable water sources [1], [2]. Magnesium is usually the limiting factor for struvite precipitation, but the high influent Mg concentration increases the probability of struvite precipitation at CVWRF [1].

Another factor for struvite precipitation at CVWRF is ammonia nitrogen, which is in high concentration in the anaerobic digester filtrate that is continually recirculated from the dewatering process back to the headworks. Utah State University and WesTech Engineering constructed and erected a pilot-scale rotating algal biofilm reactor (RABR) to remove N and P from the filtrate by cultivating microalgae growth and harvesting the biofilm periodically.

Microalgae biofilm growth removes N and P from wastewater through metabolic activity to form microalgae with the general stoichiometry of $C_{106}N_{16}P_1$ [3]–[6]**.** RABRs utilize this phenomenon through controlled microalgae biofilm growth and have treated municipal, petrochemical, and produced wastewater [7].

Nitrogen and phosphorus concentrations were reduced significantly while using a RABR system for petrochemical and municipal wastewater treatment. While using a RABR system to treat petrochemical wastewater, nitrogen, phosphorus, and total suspended solids (TSS) were reduced by up to 18.1 mg/L (72.4%), 1.00 mg/L (55.6%), and 23.9 mg/L (61.3%), respectively [8]. While using a RABR system for nutrient removal from municipal wastewater, total dissolved nitrogen was reduced from 8.3 mg/L

to 1.1 mg/L and total dissolved phosphorus was reduced from 4.1 mg/L to 1.1 mg/L. Biofilm growth was advantageous over suspended growth because biofilm achieved higher nutrient removal efficiency and biofilm was less costly to harvest. Harvested biomass can be converted in valuable bioproducts. Increasing hydraulic retention time (HRT) would likely have increased nutrient removal efficiency of the RABR system. [9] Because of previous success with N and P removal, a RABR system was chosen for a pilot study at CVWRF to meet new N and P effluent levels.

During RABR operation at CVWRF, potential struvite crystals were observed in the biofilm, shown in Figure 1. The trapezoidal crystals, ranging from approximately 20-120 μm in length, match the relative size and morphology of struvite [10], [11]. Struvite crystals appeared to correlate with biofilm growth.

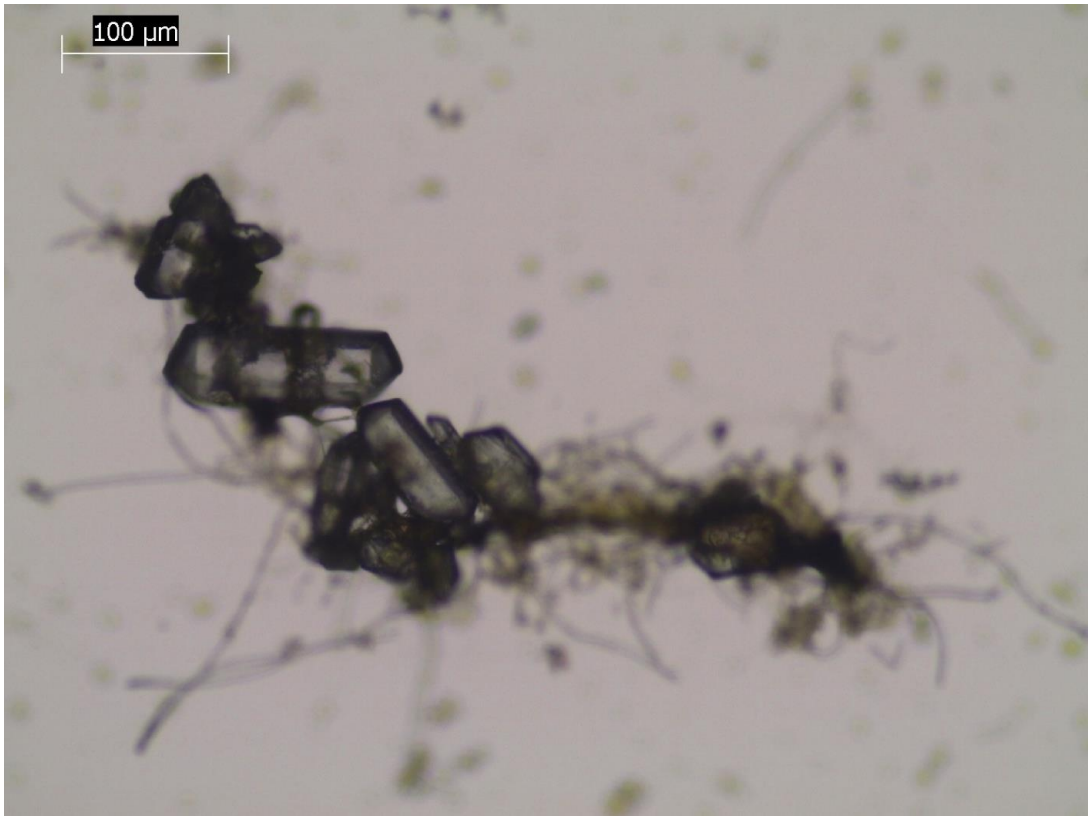

Figure 1. CVWRF RABR microalgae biofilm under 10X magnification shows apparent trapezoidal-shaped struvite crystals embedded in filamentous growth.

There are many potential factors for struvite formation in the microalgae biofilm: TS, ash content, diatom concentration, microalgae bioconsortia, biofilm development time, sun-induced evaporation, and struvite-containing sludge buildup in the biofilm. Struvite, calcium phosphate, and other Mg and Ca precipitates are possible within the RABR system because RABR influent contains N, P, Ca, and Mg. It is important to quantify struvite content and precipitate purity in the biofilm and settled tank sludge.

Studying different harvesting interval biofilm layers may help understand how development time, sun exposure, and species composition influence struvite precipitation.

Evaluating differences between east-facing vs west-facing biofilm growth may help understand how sun-induced evaporation and species composition influence struvite content of the biofilm. Comparing precipitates in the biofilm to precipitates in the sludge may help understand how the microalgae biofilm influences precipitate formation compared to natural precipitation in the RABR tank water.

Biofilm-mediated struvite precipitation could enhance N and P removal from magnesium-rich wastewater as an alternative to side-stream processes. Struvite is marketed as a slow-release fertilizer [12]. Thus, struvite in the biofilm matrix could enhance fertilizer qualities and marketability of microalgae biomass that is pelletized into fertilizer. The objective of this study is to observe, quantify, and understand struvite formation within microalgae biofilm in the CVWRF RABR system.

Materials and Methods

CVWRF RABR

The pilot-scale CVWRF RABR consisted of rotating disks inoculated with trickling filter microalgae biofilm collected from CVWRF. To inoculate the disks, trickling filter microalgae was rubbed over the disk surface. RABR influent consisted of anaerobic digester effluent filtrate (filtered using a belt press) and belt press wash water. During operation, 40% of each disk was immersed in the water while 60% was exposed to air as the disks continually rotated. The RABR operated outdoors under full sun with the disk faces oriented east and west. Over time, the inoculum spread and grew over the surface of the disks to form a biofilm. The pilot-scale RABR is shown in Figure 2**.**

Figure 2. This is the west-facing side of the CVWRF RABR. AD filtrate flows into the white settling tank on the left side then flows into the blue RABR tank.

RABR operation started October 30, 2017. Data for this project was collected June 11, 2019 to August 30, 2019, which is after 1 year and 8 months of continuous RABR operation. Table 1 summarizes RABR operational parameters.

Table 1. Operating parameters and description of the CVWRF RABR system

RABR Parameter	Description
Tank volume	4500 L (3 m Length x 1.5 m Width x 1 m Depth)
Disk arrangement	10 total: 5 disks on each of 2 shafts
Center shafts	2 shafts of 2-inch stainless steel
Disk diameter	1.2 m
Disk rotation speed	Approx. 1 revolution per minute (RPM)
Hydraulic retention time (HRT)	3.6 ± 1.2 hours
Influent to the RABR	Belt press filtrate and wash water
Average influent Total Kjeldahl Nitrogen concentration*	470 mg/L
Average influent phosphorus concentration*	24 mg/L
Average influent magnesium concentration**	50 mg/L
Average influent calcium concentration**	92 mg/L

*Average values from CVWRF laboratory, measured four times per month from January to April 2018

**Values from June 24 and September 30, 2019 measured using ICP-MS

Temperature and pH of RABR tank water and biofilm were measured using a Mettler-Toledo FiveGo portable pH and conductivity probe, calibrated daily. Temperature, pH, and samples of biofilm and RABR water were collected between 10 am and 5 pm weekly. pH values were converted to hydrogen ion concentration (M) using the equation $pH = -log[H^+]$. The hydrogen ion concentration was averaged then converted back to pH using the same equation. Photosynthetically active radiation (PAR) from sunlight was continuously monitored over time using a LI190R Quantum Sensor (LI-COR) and Campbell Scientific datalogger.

Comparison of Magnesium, Calcium, and Phosphorus content of RABR Settled Sludge, Microalgae Biofilm, and Inoculum

Magnesium, calcium, and phosphorus mass content and molar ratios were compared for the RABR settled sludge, biofilm, and biofilm inoculum (trickling filter microalgae). Samples of RABR settled sludge, biofilm, and inoculum were collected, dried, powdered, and dissolved in 1 N sulfuric acid. The samples were then vortexed and sonicated for 10 minutes twice to ensure Mg, Ca, and P were completely dissolved. The pH of solutions ranged from 1.1 to 1.7. The samples were diluted to 1:100 in deionized (DI) water and analyzed via inductively coupled plasma mass spectrometry (ICP-MS) by the Utah Water Research Laboratory (UWRL).

Struvite Observation and Quantification in the Harvesting Interval Layers of East and West RABR Microalgae Biofilm Matrix

The RABR disks were inoculated with biofilm collected from trickling filters at CVWRF. Light microscope images and species composition of the inoculum is included in the Chapter 1 Appendix (Figure 20). There was no struvite observed in the inoculum.

Three RABR microalgae biofilm harvesting intervals were evaluated: 1-week growth (top layer), 2.5-month growth (top layer), and the bottom layer that developed over a 2.5-month period. The bottom layer was left as inoculum for each growth cycle when the biofilm was harvested weekly. Maintaining a healthy bottom layer of cells in the microalgae biofilm is critical for each weekly growth cycle [13]. Figures 3 and 4 depict the microalgae biofilm harvesting interval layers on the east and west-facing RABR disks.

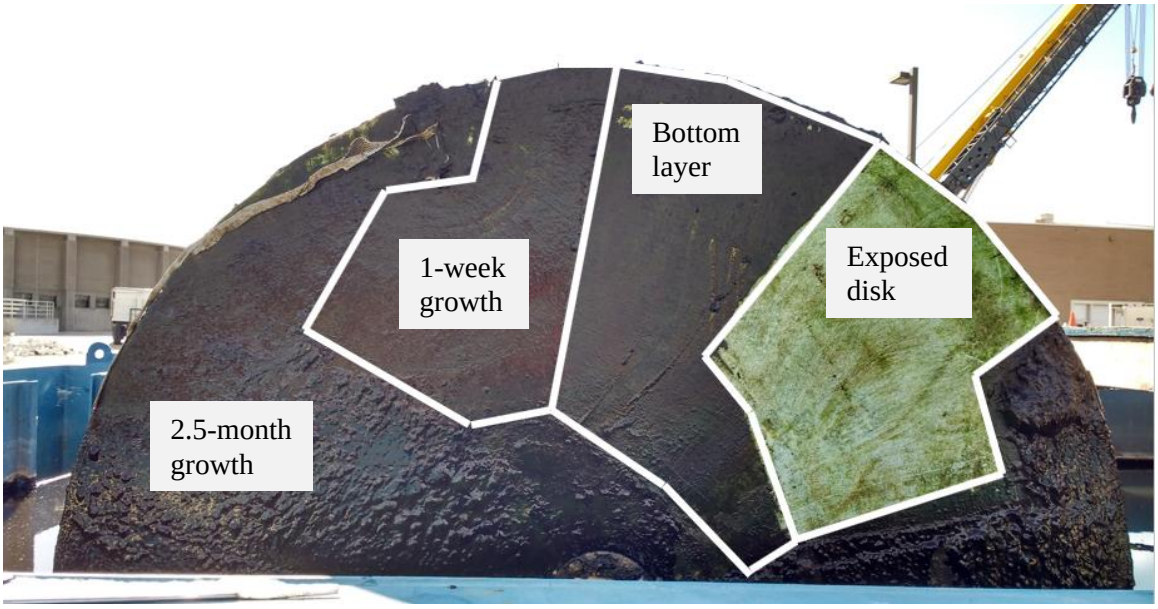

Figure 3. The east-facing disk of the CVWRF RABR showing the three harvesting interval layers evaluated in this study

(a)

(b)

Figure 4. The west-facing disk of the CVWRF RABR showing **(a)** the bottom layer of cells and **(b)** one week later that was used for sampling in this experiment.

Images of the inoculum, biofilm layers, and ash were captured using a light microscope (Leica DM 750) and high-resolution digital camera (Leica ICC 50) to visualize struvite crystals, biofilm species composition, and biofilm health. A "healthy" biofilm has higher microalgae content, species variation, and is greener in color than a less healthy biofilm. Scanning Electron Microscopy (SEM) and Energy Dispersive X-Ray Spectroscopy (EDS) was performed by the Utah State University Office of Research, Microscopy Core Institute to visualize and confirm struvite crystals in the biofilm.

Nutrient Analysis of Ash

Total solids (TS) were determined using Method 2540 B, and volatile solids (VS) and ash were determined using Method 2540 E from Standard Methods 21st Edition [14]. Total solids were calculated from initial wet mass. Struvite, diatom cell walls, and other inorganics will remain after volatilization [14], [15].

Ash was weighed and collected in a 100 mL volumetric flask. Five milliliters of 1N sulfuric acid was added to the volumetric flaks and swirled to dissolve phosphate precipitates in the ash. Deionized water was added up 100 mL. Sample pH within the volumetric flask was approximately 1 for all samples. Samples were stored at 4°C but brought to room temperature for analysis.

Struvite is the only potential phosphate precipitate that contains ammonium; thus, ammonium concentration in the ash accurately quantifies struvite concentration in the biofilm [5], [16]. Total nitrogen was measured instead of ammonia because of potential interferences with the ammonia method. Interferences of concern with the ammonia method include Ca (50,000 mg/L as $CaCO_3$), Mg (300,000 mg/L as $CaCO_3$), pH (alkaline

or acidic), phosphate (5000 mg/L as PO_4^{3-}P), and sulfate (6000 mg/L as SO_4^{2-}) from the sulfuric acid digestion. Measuring total N is acceptable because ammonium in the struvite is the only N expected in the ash. Organic N was volatilized during ashing. Total nitrogen concentration was measured using HACH Persulfate Digestion HR Test 'N Tube™ (Method 10072). ANOVA was used to determine significance of TS, ash, and struvite content between biofilm layers.

Total P, Mg, and Ca was measured using Inductively Coupled Plasma - Mass Spectroscopy (ICP-MS) by the Utah Water Research Laboratory. Ratios of Mg, Ca, and P in the ash approximates the purity of struvite compared other potential phosphate precipitates in the biofilm layers. Precipitates dominated by struvite will contain approximately equimolar Mg and P with little Ca. Higher Ca content indicates potential calcium phosphate in the precipitates.

Results and Discussion

Temperature and pH of RABR Tank Water and Biofilm

The most critical variables in struvite precipitation is pH and supersaturation of magnesium, ammonium, and phosphate [16]–[19]. RABR water and biofilm pH is shown in Table 2 with an average tank water pH of 7.9 and average biofilm pH of 8.0. There can be 80% P recovery as struvite when pH is 7.9 if the molar concentration of Mg:P is 1.5:1 or greater. Increasing pH in the range of 7.9 to 8.4 reduces the required Mg:P ratio for struvite precipitation. [20] Struvite precipitation potential increases exponentially as pH increases in this range [18]. The molar ratio of Mg:Ca:P of settled influent supernatant is

3.8:4.2:1 (46 mg/L Mg, 87 mg/L Ca, and 14 mg/L P), which has potential for both magnesium and calcium phosphate precipitates [10], [16].

Doyle and Parsons (2002) claim calcium phosphate precipitation occurs above pH 9.5, which is above any measured pH in the RABR system (Table 2). J. Wang et al. (2005) found calcium precipitates at pH 7.8 when Ca concentration was high and Mg:Ca molar ratio was 1:1. The pH and temperature range in the RABR biofilm and water (Table 2) are favorable to struvite precipitation with possible calcium precipitates [10], [16], [18], [20], [21]**.** Data and calculations for Table 2 are in the Chapter 1 Appendix (Tables 5-7).

Table 2. Temperature and pH statistics of RABR tank water and microalgae biofilm

		Average	Minimum	Maximum	Standard Deviation	Coefficient of Variation (%)
Tank Water	pH	7.9	7.2	8.1	0.23	2.9
	°C	26	21	29	2.2	8.4
Biofilm	pH	8.0	7.9	8.4	0.11	1.3
	°C	25	22	31	2.6	10

n = 30

Though not statistically significant, RABR biofilm pH was measurably higher than water pH. Photosynthesis of microalgae consumes carbon dioxide (CO_2) and bicarbonate (HCO_3^-), significantly increasing pH of the growth medium [22], [23]. The same phenomenon is likely happening within the biofilm matrix.

At a disk rotation of approximately 1 RPM, the biofilm is continually saturated by

RABR water. As such, RABR water may influence the pH probe reading of the biofilm. It is possible the pH is significantly higher at the cellular interface than was detected.

Magnesium, Calcium, and Phosphorus content of RABR Settled Sludge, Microalgae Biofilm, and Inoculum

The key findings from Table 3 focus on the mass balance and molar ratios of Mg, Ca, and P throughout the biofilm, inoculum, and sludge. Mass accumulation of Mg and P in the biofilm is 113.4 g kg^{-1} (94% increase) and 157.8 g kg^{-1} (93% increase), respectively, which was found by subtracting Mg and P inoculum mass from biofilm mass (Biofilm minus Inoculum in Table 3). The mass accumulated in the biofilm has a Mg:P molar ratio of 0.92:1, which is close to the expected 1:1 molar ratio of struvite. Mg and P sludge mass was subtracted from Mg and P mass accumulated in the biofilm to ensure Mg and P mass accumulation was not due to sludge buildup (Biofilm minus Inoculum minus Sludge in Table 3). Data and calculations for Table 3 are in the Chapter 1 Appendix (Tables 8-10).

Table 3. Magnesium and phosphorus concentration as a function of dry weight for RABR biofilm inoculum (trickling filter microalgae), biofilm, and settled sludge. The coefficient of variation is <1 for all relevant replicates.

Sample	g Mg kg^{-1} Sample	g Ca kg^{-1} Sample	g P kg^{-1} Sample	Mg:Ca:P (Molar)
Inoculum[1]	7.4 ± 0.6	28.6 ± 4.1	10.5 ± 0.6	0.9:2.1:1
Biofilm[2]	120.7 ± 18	24.8 ± 14	168.3 ± 19	0.9:0.1:1
Sludge[2]	9.8 ± 0.8	43.9 ± 5.8	23.6 ± 1.6	0.5:1.4:1
Biofilm minus Inoculum	113.4	-3.8	157.8	0.92:-:1
Biofilm minus Inoculum minus Sludge	103.5	-47.7	134.2	0.98:-:1

[1]Averaged duplicates ± standard deviation
[2]Averaged triplicates ± standard deviation

Results show Mg and P mass accumulation is not due to sludge buildup. Mass accumulation of Mg and P in the biofilm is 103.5 g kg^{-1} (86% increase) and 134.2 g kg^{-1} (79% increase), respectively, after subtracting the potential contribution of sludge buildup. The Mg:P molar ratio of mass accumulated in the biofilm is 0.98:1 when sludge is subtracted. If sludge is accumulating in the biofilm, sludge is not significantly contributing to struvite. Also, the 0.98:1 Mg:P molar ratio after sludge is subtracted is closer to the 1:1 molar ratio of struvite present in the biofilm. Calcium is not a constituent of struvite, and Table 3 indicates that Ca mass is lost in the biofilm.

Table 3 indicates the biofilm has lower Ca mass content than the inoculum. Mass loss of Ca could be attributed to solubilization and precipitation of Ca into the sludge, indicated by the negative values in Table 3. Molar ratios of Mg, Ca, and P from literature indicate that struvite is likely accumulating in the biofilm while calcium phosphate may

be precipitating in the sludge. This data was indicative of struvite accumulation in the biofilm, but struvite content cannot be accurately quantified without nitrogen content of precipitates. Additionally, the microalgae biofilm varies based on sun exposure and harvesting interval, which could impact struvite content.

RABR Microalgae Biofilm Harvesting Interval Layers

Different harvest interval layers and east/west sun orientation of the biofilm are expected to have slightly different species composition due to species photosensitivity [24]–[26]. PAR values at the CVWRF RABR reached up to 47,500 $\mu mol \cdot m^{-2} \cdot s^{-1}$ with average PAR of 37,000 $\mu mol \cdot m^{-2} \cdot s^{-1}$. Photoinhibition has been observed above PAR values of 500 $\mu mol \cdot m^{-2} \cdot s^{-1}$ in various microalgae species [24], [25].

The top layers of growth (1-week and 2.5-month) were exposed to direct sunlight. West had more direct sun exposure with higher intensity because of afternoon sun, while east only experienced direct sunlight in the morning. The top cell layers likely consist of species adapted to higher light intensity, and top cell layers may have a shading effect on the bottom cell layers. The shading effect may increase photosynthesis and allow more photosensitive growth in the bottom layer [24]. Roberts et al. (2004) states new colonization is expected to have high levels of diatoms that will become intermixed within the biofilm matrix as the algal community develops, which was observed in Figures 5-7. There could be more evaporation in the west biofilm due to sun exposure, which could supersaturate magnesium, ammonium, and phosphate to favor struvite precipitation.

Microalgae Biofilm Bottom Layer

The bottom layer of the east-facing RABR disk (Figure 5a,b) appears to have more struvite, *Chlorella*, and filamentous growth than other layers of the east biofilm (Figures 6 and 7). Figure 5 indicates the highest struvite content and most biodiversity in the bottom layer compared to other layers of the east biofilm. The east bottom layer has less diatoms and the most filamentous growth and *Chlorella* compared to other east and west layers. Struvite crystals correlate with biomass as opposed to diatom content.

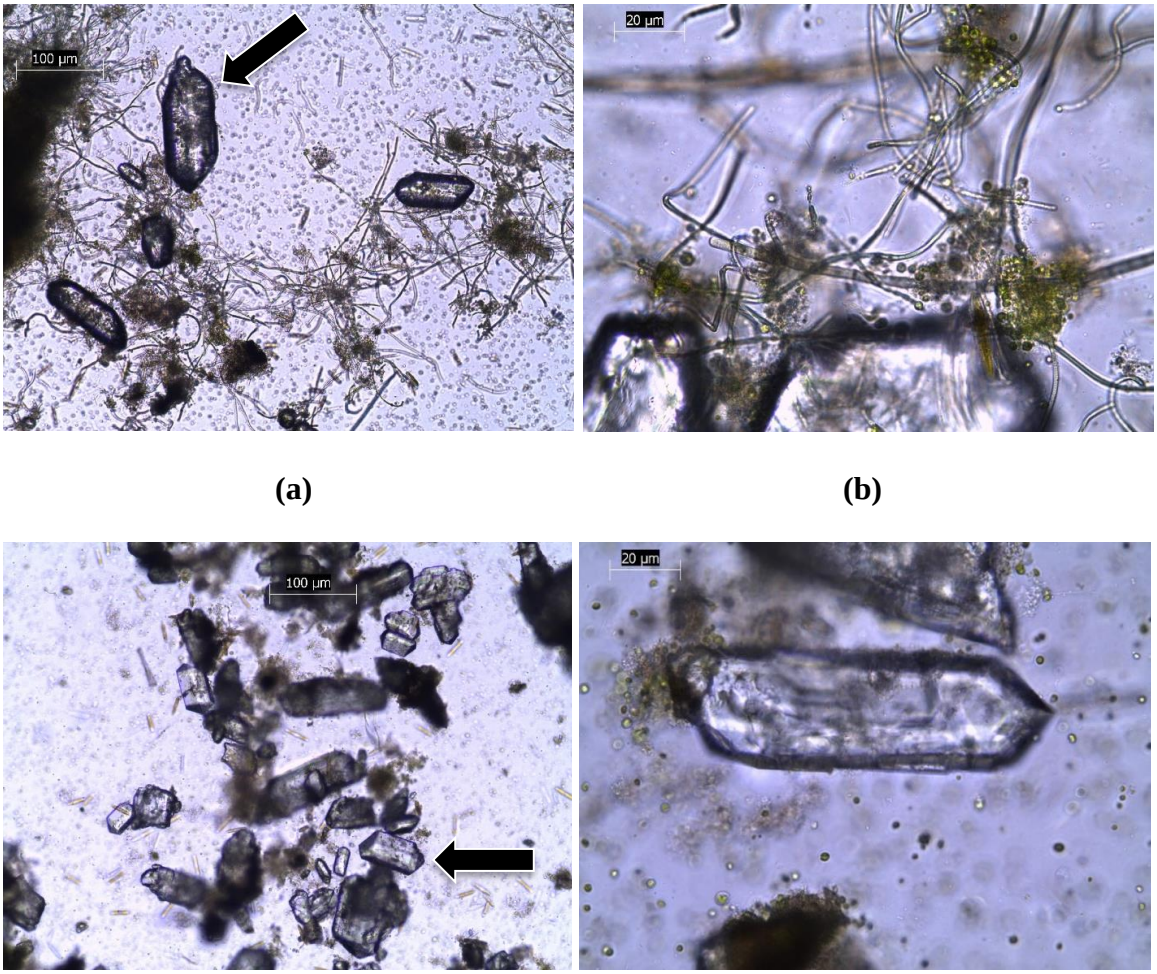

Figure 5. The bottom layer of the east biofilm magnified at 10X **(a)** and 40X **(b)** shows *Chlorella*, filamentous microalgae and cyanobacteria, diatoms, and struvite crystals. Struvite in the east bottom layer appear to be entangled in *Chlorella* and filamentous growth. The bottom layer of the west biofilm magnified at 10X **(c)** and 40X **(d)** shows *Chlorella*, diatoms, and struvite crystals. The west bottom layer has no visible filamentous growth. Struvite correlates with *Chlorella*, as seen in **(d)** with the green dots attached to the crystal. Arrows indicate a struvite crystal.

Like the east biofilm, the bottom layer of west biofilm (Figure 5c,d) has more *Chlorella* and filamentous growth with less diatoms than other west layers. The upper layers of the west biofilm may shade the bottom layer, allowing more algal and cyanobacterial growth. Struvite content appears higher in the west bottom layer of light microscope images compared to other west layers (Figure 6 c,d and Figure 7 c,d).

The bottom layers of the east and west microalgae biofilms have higher apparent struvite content and more microalgae than other layers. The bottom layer is shaded by the top layers, which could reduce photoinhibition and increase microalgae content and biodiversity. The higher struvite content in the bottom layers could be directly correlated to the higher microalgae content.

Microalgae Biofilm One-Week Growth

East 1-week growth in Figure 6a,b contains diatoms, *Chlorella, Oscillatoria,* and *Pseudoanabaena* [14], [27]. East 1-week growth has high struvite content embedded in the biofilm. The filamentous microalgae and cyanobacteria, diatoms, and *Chlorella* form a matrix that appears to correlate with struvite.

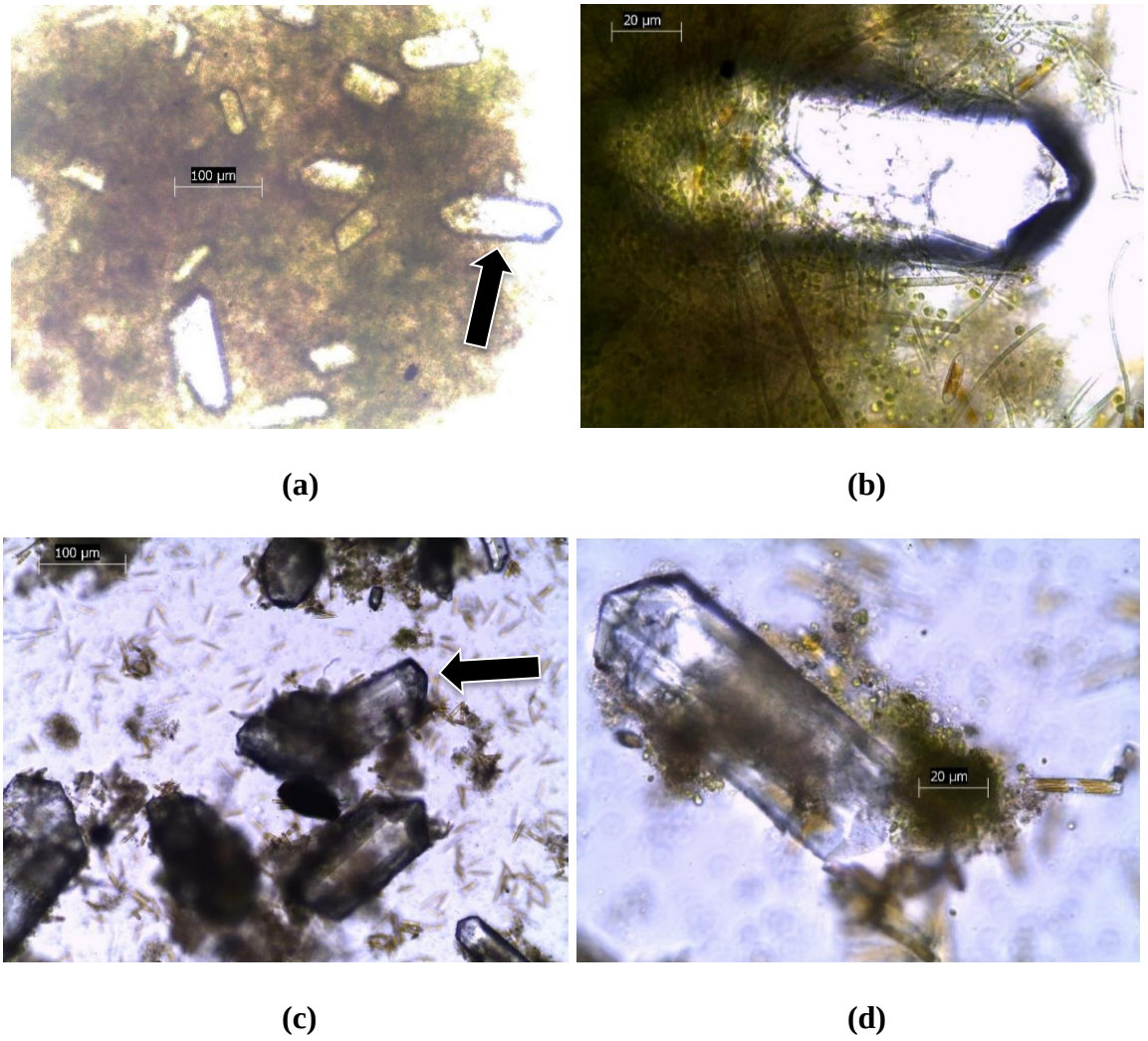

(a) **(b)**

(c) **(d)**

Figure 6. East 1-week growth magnified at 10X **(a)** and 40X **(b)** show struvite crystals embedded in the mixed microalgae biofilm matrix that contains *Chlorella*, diatoms, *Oscillatoria*, and *Pseudoanabaena*. West 1-week growth magnified at 10X **(c)** and 40X **(d)** show struvite crystals associated with *Chlorella*. Diatom content appears high in west 1-week growth. Arrows indicates a struvite crystal.

West 1-week growth (Figure 6c,d) also has high struvite content. West 1-week growth has less filamentous growth than east, but struvite appears to correlate with clusters of *Chlorella* and brown scum. Brown scum could be sludge breakthrough from

the anaerobic digesters, stained *Chlorella*, or stained biofilm matrix. Filamentous growth is less prevalent in west 1-week growth potentially because the light intensity throughout the day is too high compared to the east [24]. *Chlorella* can withstand higher light intensity [26].

Figure 6 shows 1-week growth has different species composition when east vs west-facing. East 1-week growth experiences direct sunlight only in the early hours of the day while the west experiences direct sunlight throughout the afternoon and evening. East 1-week growth appears to promote more filamentous growth compared to west. The resulting east biofilm matrix appears to have high struvite content within the biofilm.

Microalgae Biofilm 2.5-Month Growth

East 2.5-month growth (Figure 7a,b) mostly consists of diatoms and brown scum. Struvite, *Chlorella*, and filaments are present at lower concentration than other east biofilm layers. Struvite appears at lower concentration likely because there is less biofilm matrix to interface with. The high diatom content and low struvite content further indicate a lack of correlation between diatoms and struvite.

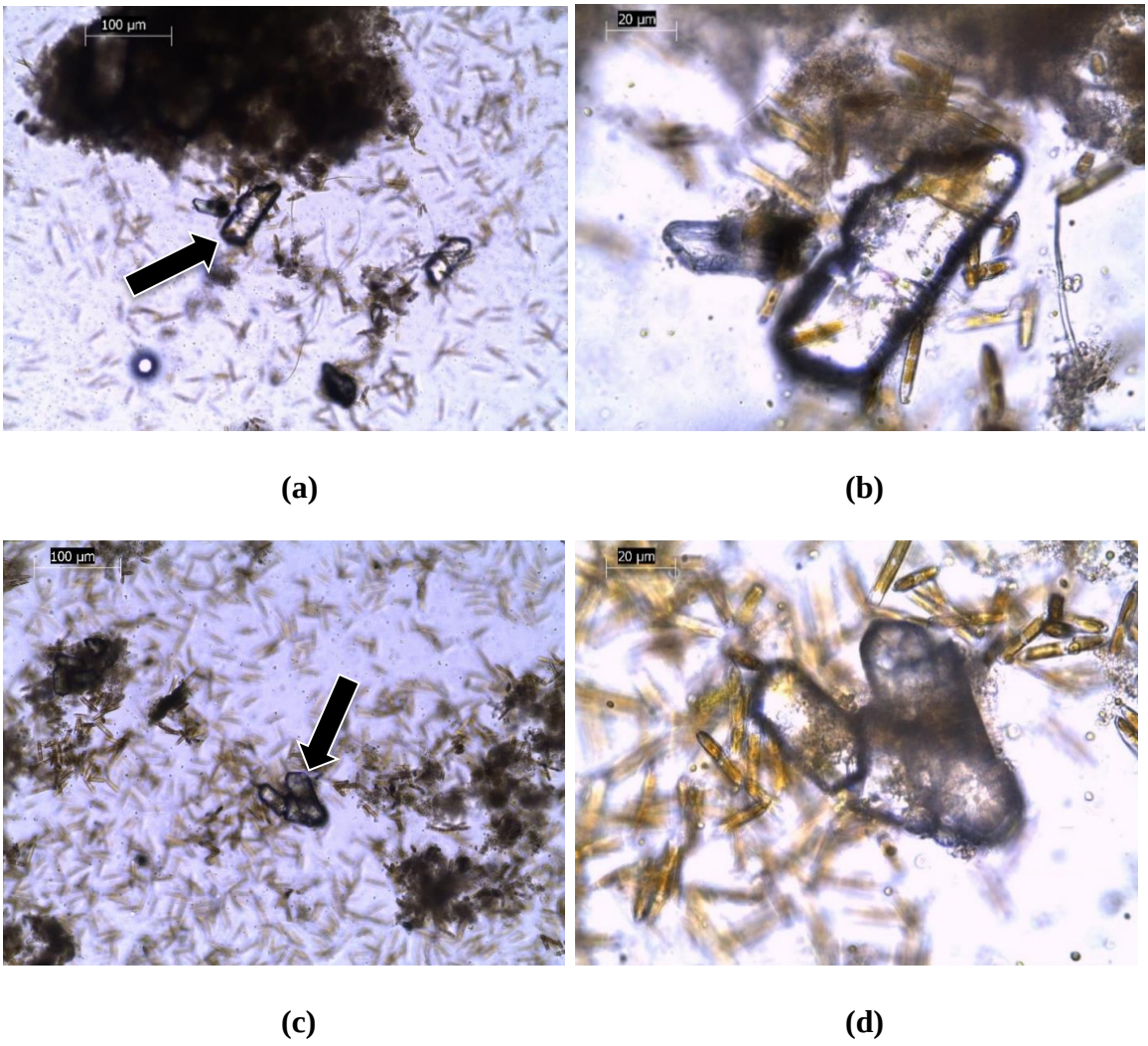

Figure 7. East 2.5-month growth magnified at 10X **(a)** and 40X **(b)** show struvite scattered throughout the biofilm with little filamentous growth or *Chlorella* but abundant brown scum and diatoms. West 2.5-month growth at magnified at 10X **(c)** and 40X **(d)** show struvite visible in the brown scum, abundant diatoms, no filamentous growth, and little *Chlorella*. Arrows indicate a struvite crystal.

West 2.5-month growth (Figure 7c,d) is also dominated by diatoms and brown scum. Struvite, and *Chlorella* are present in lower quantities than other west biofilm

layers with no filamentous growth. Sun overexposure may prevent the development of a healthy biofilm, or most of the microalgae dies and decomposes as the biofilm ages. East and west 2.5-month growth have similar apparent bioconsortia and struvite content.

SEM/EDS Imaging

The use of SEM/EDS verified struvite is the crystal observed in the light microscopy images in Figures 5-7. Struvite is not the only possible precipitate; calcium and other magnesium precipitates are possible in the measured pH range of RABR water and biofilm [5], [10], [16], [20]. Figure 8a shows an SEM image of east RABR biofilm with struvite crystals. EDS rendering of the crystals (Figure 8b-d) indicate that magnesium and phosphorus are the primary crystal constituents, while calcium is not. Therefore, the crystals in Figures 5-7 are struvite. Additionally, crystals match the expected size and morphology of struvite [10], [16].

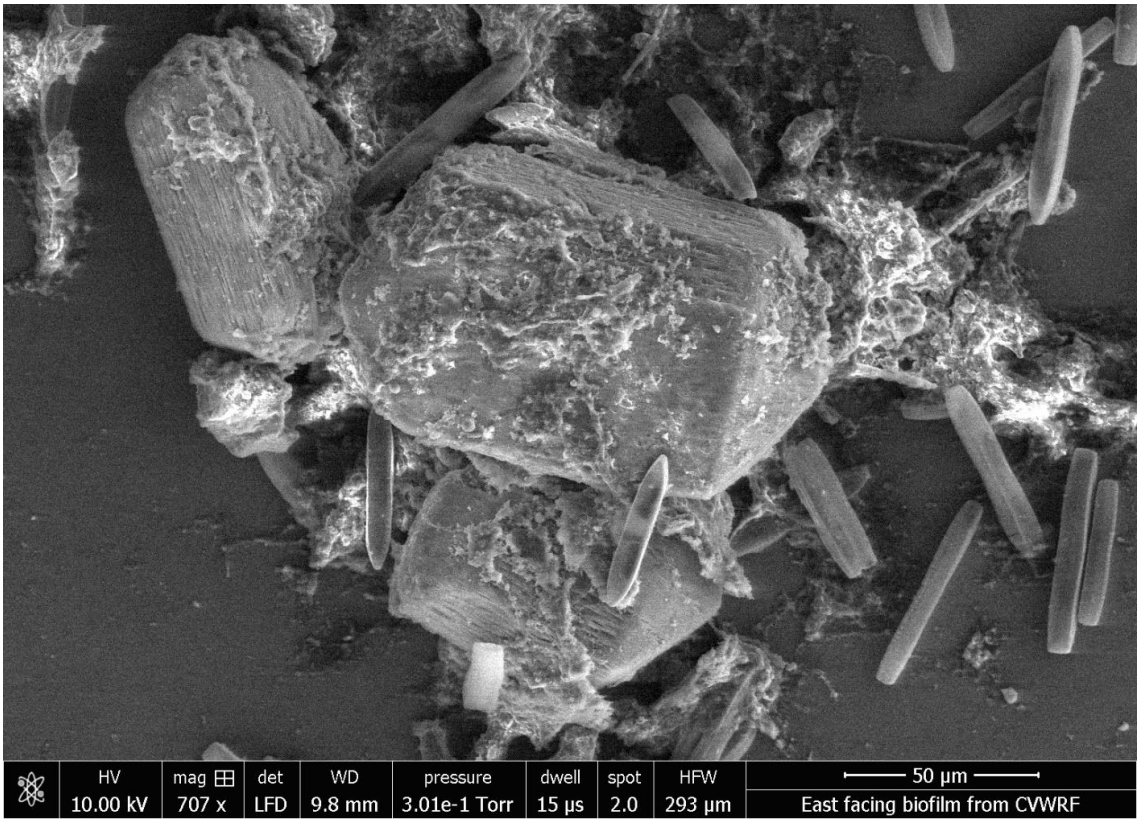

(a)

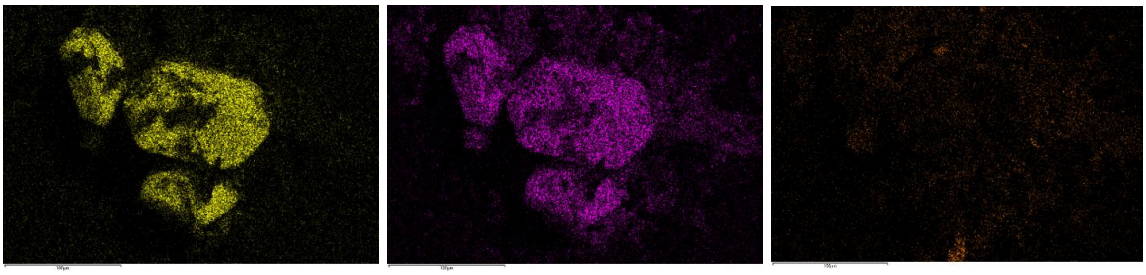

(b) **(c)** **(d)**

Figure 8. (a) shows struvite crystals from the east biofilm imaged using SEM. The three larger crystals embedded in the biofilm are struvite while diatoms are the smaller crystal-like forms. EDS rendering shows that the atomic signatures of Mg **(b)**, P **(c)**, and Ca **(d)** in the three large crystals match the 1:1 molar ratio of Mg:P expected in struvite. There is no Ca signature in the three crystals, so they cannot be calcium phosphate.

The map sum spectrum for atomic percentage in Figure 9 further indicates the observed crystals are struvite. Phosphorus, nitrogen, and magnesium make up approximately 2.7%, 2.3%, and 2.3%, respectively, of the total atomic percentage in the SEM image (Figure 8a). Phosphorus, nitrogen, and magnesium are approximately equimolar, which is expected for struvite.

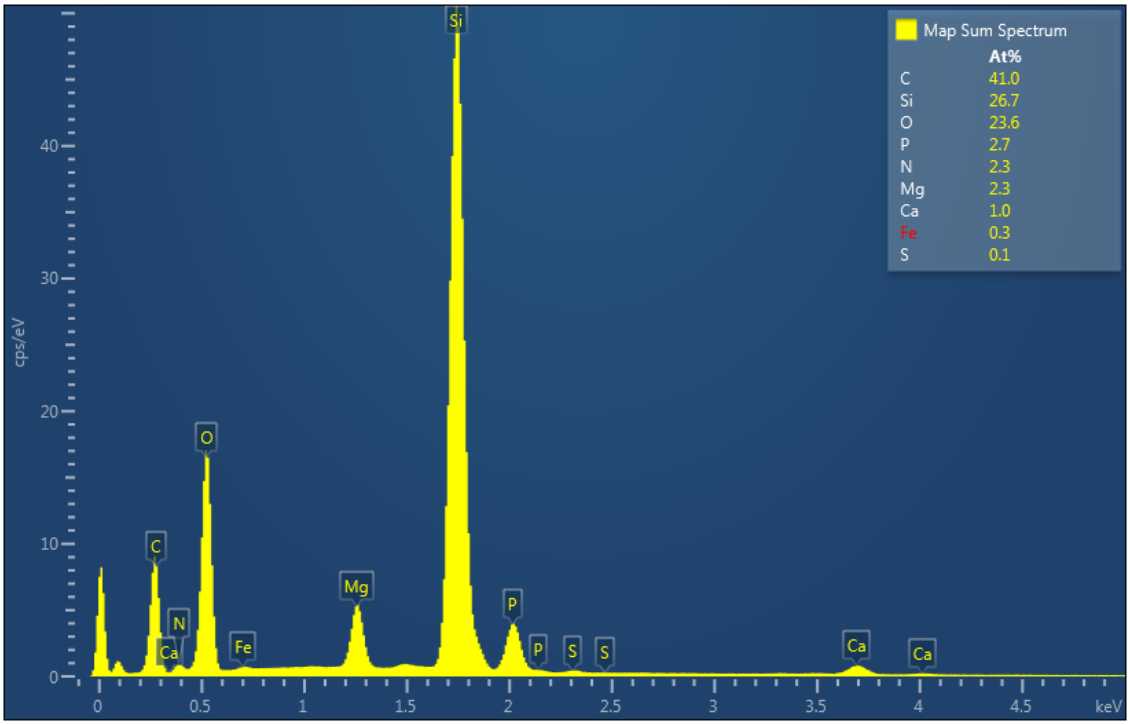

Figure 9. The map sum spectrum after EDS rendering of the SEM image in Figure 5a shows the atomic percentage (At%) of phosphorus (P), nitrogen (N), and magnesium (Mg) are approximately equimolar. Carbon (C), silicon (Si), and oxygen (O) are inaccurate due to environmental interferences and the silica chip the sample was placed on for SEM/EDS.

Nutrient Analysis of RABR Inoculum and Biofilm Ash

Ashing the biofilm eliminated organics that may contain Mg, Ca, N, and P that interfere with struvite quantification. Figure 10 shows a light microscope image of biofilm ash to verify struvite presence. Wang and Seibert (2017) demonstrate that diatoms contain almost 33% ash, likely from the diatom silica cell wall [28]. Biofilm ash mainly consists of diatom silica cell walls and struvite.

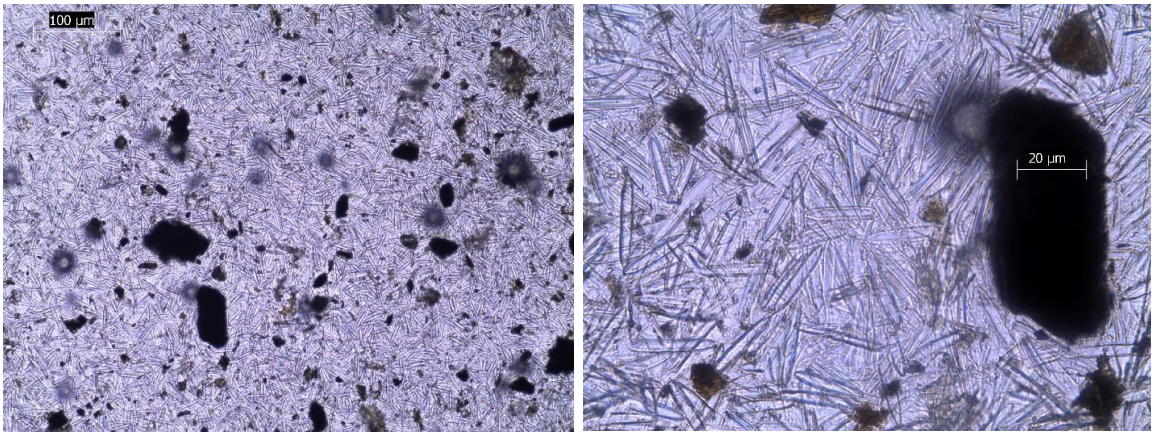

(a) **(b)**

Figure 10. Biofilm ash magnified at 10X **(a)** and 40X **(b)** show struvite (black forms) on a background of diatom silica cell walls. The black form that contains the scale bar **(b)** matches the expected size and morphology of struvite compared to Figures 5-7.

Struvite content was quantified by measuring total nitrogen in the ash and translated to a mass percent of TS, shown in Figure 11. Comparative figures of TS and ash are included in Figure 12. Data and ANOVA for Figures 11 and 12 are in the Chapter

1 Appendix (Tables 11-12 and Tables 13-15, respectively).

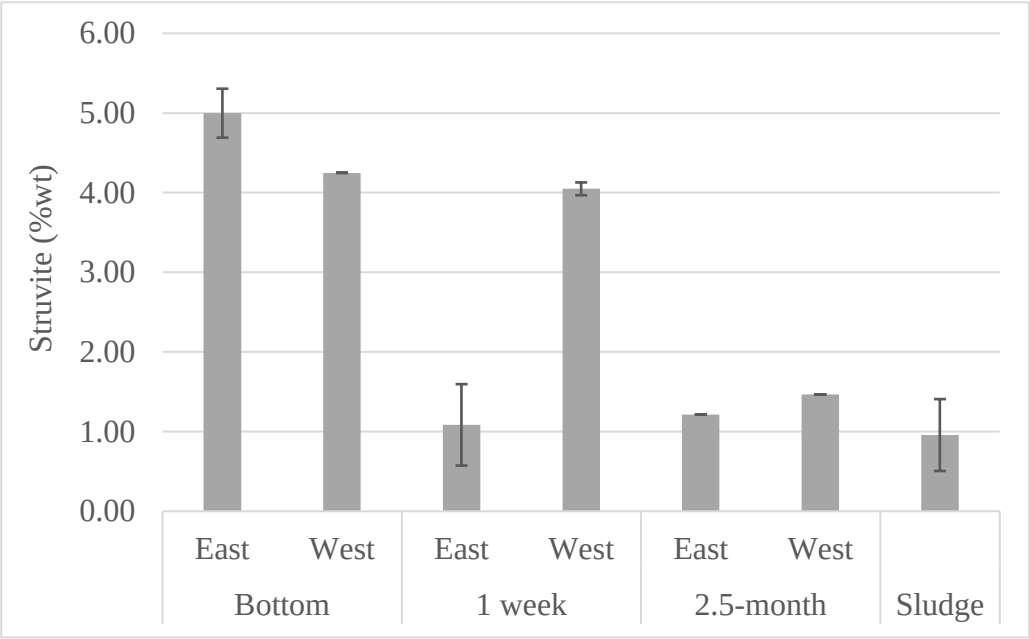

Figure 11. Struvite is expressed as percent mass of TS. The bottom layer of cells in the biofilm is labeled "Bottom," 1-week growth labeled "1 week," and 2.5-month growth labeled "2.5-month." The inoculum is labelled "TF" for trickling filter. "Sludge" is settled sludge from the RABR tank.

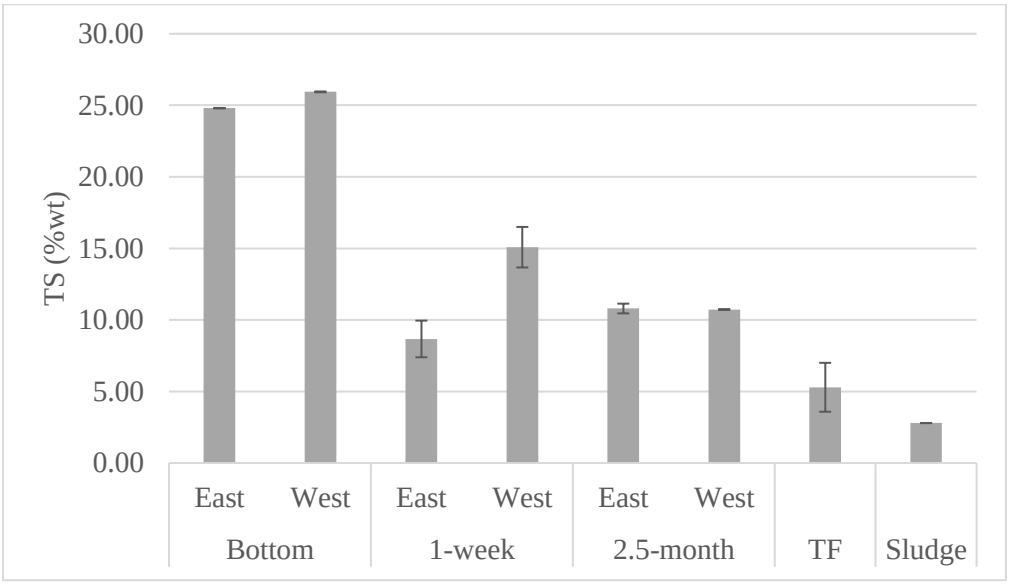

(a)

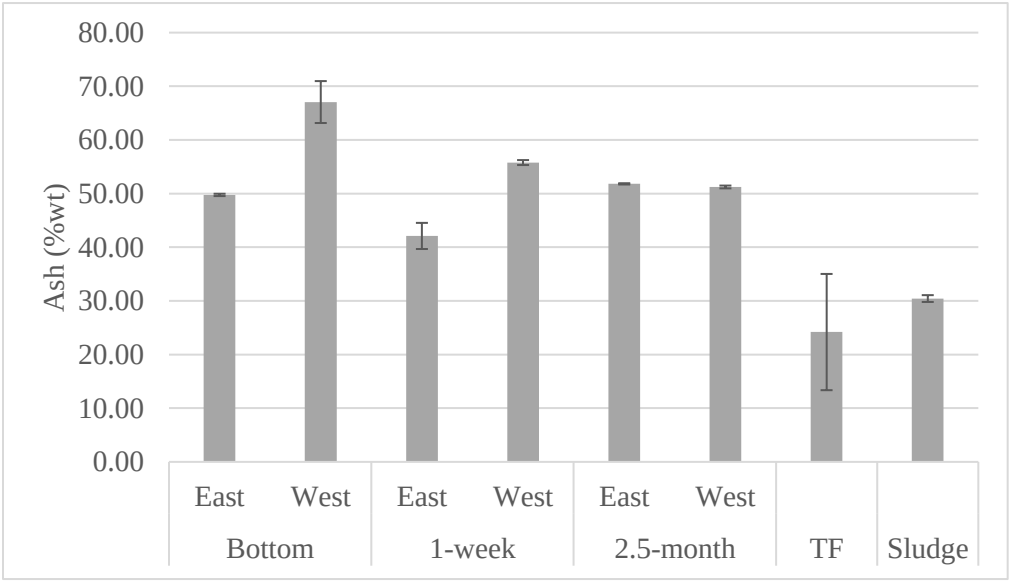

(b)

Figure 12. TS is expressed as percent mass of wet biomass. Ash is expressed as percent mass of TS. The bottom layer of the biofilm is labeled “Bottom,” 1-week growth labeled “1-week,” and 2.5-month growth labeled “2.5-month.” The inoculum is labelled “TF” for trickling filter. “Sludge” is settled sludge from the RABR tank.

The bottom layer of biofilm has higher TS than other layers. The east bottom layer has lower TS and ash than the west bottom layer, but east/west bottom and west 1-week do not have significantly different struvite levels. The higher ash content of west bottom is likely attributed to diatoms instead of struvite.

Struvite content and TS of east 1-week growth is not significantly different from east or west 2.5-month growth, but significantly lower than the bottom layers. West 1-week growth has significantly more TS, ash, and struvite than east. Struvite content of west 1-week growth is not significantly different from west bottom growth. TS and Ash of west 1-week growth is second highest compared to other west layers.

Ash content in east 2.5-month growth is higher than other east layers likely from diatoms. Struvite and TS of east 2.5-month growth is significantly lower than east bottom growth but not significantly different from east 1-week growth. Struvite, TS, and ash in 2.5-month growth are not significantly different between east and west. Struvite, TS, and ash is lowest in west 2.5-month growth compared to other west layers.

The highest struvite content on the east is the bottom layer of growth. Figure 6a,b shows high struvite content within east 1-week biofilm matrix, but Figure 11 indicates east 1-week growth has similar struvite content to 2.5-month growth despite the apparent lack of healthy biofilm development in 2.5-month growth. Struvite is correlated to the biofilm matrix (Figure 6a,b), so struvite in east 1-week growth may be low because the biofilm observed in Figure 6a,b may not have had time to develop and spread. The relatively high standard deviation for struvite content in east 1-week growth could result from non-homogenous samples that consist of small biofilm clusters that contain a high

struvite content. One week may not have been a long enough development time for these clusters to create a uniform biofilm layer like the bottom layer of cells. The west bottom layer also has relatively high struvite content.

The highest struvite content on the west is 1-week and bottom growth. Figures 5c,d and 6c,d show west bottom and 1-week growth look similar with struvite correlated with *Chlorella*. However, TS and ash are higher in west bottom than 1-week growth. Therefore, TS and ash are not standalone indicators of struvite content likely due to diatom influence on TS and ash. Despite the similarity in struvite content, west 1-week and bottom growth have different development times.

Biofilm development time is not the main factor for struvite content in biofilm. Both the bottom layer and 2.5-month growth developed over a 2.5-month period, but the bottom layer had significantly more struvite than 2.5-month top-layer growth for both east and west. Additionally, both bottom and 1-week growth had relatively high and similar struvite content on the west. Evaporation from sun exposure seems to have little influence on supersaturation of magnesium, ammonium, and phosphate to precipitate struvite.

Because both 1-week and 2.5-month growth are equally sun-exposed, influences of evaporation and supersaturation should be similar when in the same sun orientation. Struvite content of east 1-week and 2.5-month growth are not significantly different and receive comparable sun exposure. However, struvite content of east 1-week and 2.5-month growth are significantly lower than east bottom layer. If sun evaporation were the main driver of struvite precipitation, expected results would be opposite.

Additionally, west 1-week and 2.5-month growth receive similar sun exposure while west 1-week growth has significantly more struvite than west 2.5-month growth. Presence of struvite, therefore, may be more correlated to biomass than evaporation. Struvite content per unit mass of biofilm may decrease from 1 week to 2.5 months because diatom content increases while microalgae content decreases. According to Figure 11, there is also struvite in the settled RABR tank sludge.

Settled RABR tank sludge has struvite content comparable to east 1-week growth and east/west 2.5-month growth. Struvite in the sludge could precipitate in the RABR water. Or, struvite may have been present in the suspended solids from AD belt press wash water, entered the RABR tank, and settled in with the sludge. Struvite is present in all microalgae biofilm growth layers and settled tank sludge, but other calcium and magnesium precipitates could also be present.

According to Figure 13, Mg and Ca molar ratios are consistent with relatively pure struvite in most biofilm layers [16]. Struvite purity is a measure of how much magnesium is present in precipitates over calcium. If the precipitates contain high magnesium with little or no calcium, the precipitates are predominantly struvite. Data and calculations for Figure 13 are in the Chapter 1 Appendix (Tables 16-18).

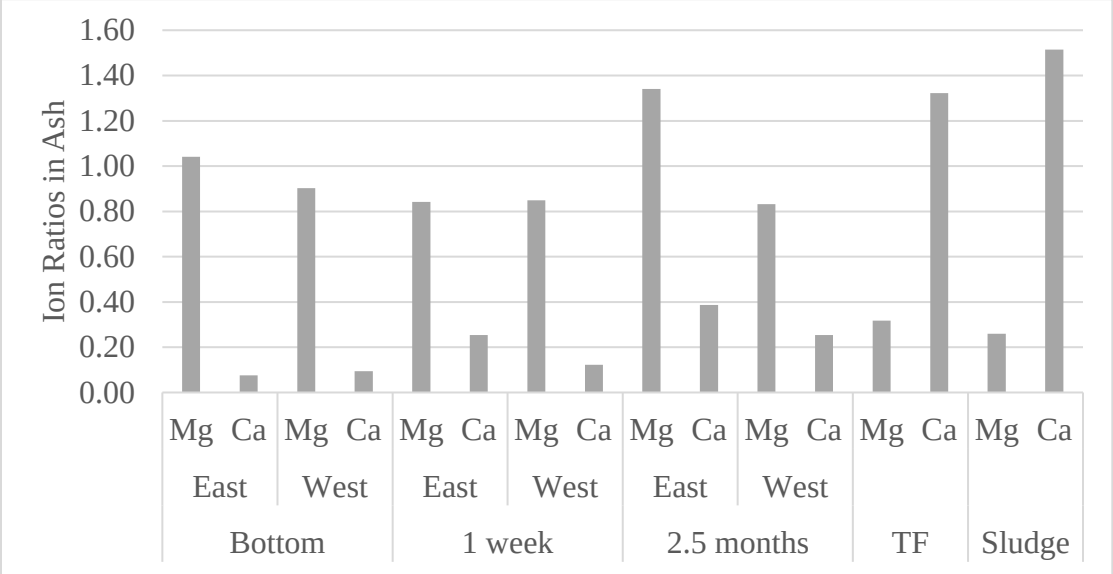

Figure 13. ICP-MS results for relative Mg and Ca molar ratios normalized to P. This graph represents the relative purity of phosphate precipitates in the 3 biofilm layers on the east and west side. The biofilm inoculum (TF) does not contain struvite, but the sludge contains some struvite.

The inoculum does not contain struvite, but calcium ratios are high. The inoculum contained almost 95% moisture, and the high calcium content in the wastewater may have reacted with phosphate in the liquid phase of inoculum to form calcium phosphate. Biofilm layers with lower TS appear to have more Ca. Thus, Ca in the ash may be due to high calcium concentration in the wastewater.

Precipitates in the bottom layer consists mainly of pure struvite for east and west. The Mg/P molar ratio is very near one in the east bottom layer, so the Ca present in the bottom layer may be baseline Ca in the biofilm or wastewater.

Calcium precipitates may be present at low quantities in east 1-week growth, but Ca does not seem above baseline levels in west 1-week growth. The precipitates in 1-

week growth are mostly consistent with pure struvite [16].

Struvite purity seems to decrease in east 2.5-month growth because precipitates have excess of over 0.3 moles of P per mole of Mg (Figure 13). Excess P is likely attributed to calcium phosphate as there is higher calcium in east 2.5-month growth. Molar ratios for Mg and Ca are similar for west 2.5-month growth and east 1-week growth. Most of the P in west 2.5-month and east 1-week growth is likely from struvite, but some calcium phosphate may be present [16]. Sludge and trickling filter precipitates contain significantly more calcium than biofilm layers.

The Ca/P molar ratios of trickling filter biofilm and sludge indicate precipitates are dominated by calcium phosphate. Though no precipitates were observed in the trickling filter biofilm, the molar ratios indicate calcium phosphate. Sludge contained struvite, but calcium phosphate concentrations appear significantly higher than struvite. Doyle and Parsons (2002) state that calcium phosphate typically precipitates when pH is 9.5 or above, but the average pH in RABR tank water was 7.9. Influent component ion concentration and molar ratios of Mg, Ca, and P are likely high enough to allow calcium phosphate precipitation at a lower pH. Calcium phosphate can precipitate at pH 7.8 when phosphate is not a limiting factor and Mg and Ca is equimolar in high concentrations [16]. RABR tank water may favor calcium phosphate over struvite precipitation without the influence of microalgae biofilm.

Despite the influent Mg:Ca:P molar concentration having potential for both struvite and calcium phosphate precipitation, the biofilm favors struvite precipitation. The biofilm mechanism that favors struvite over calcium phosphate formation is likely pH

regulation while providing nucleation sites for struvite seed crystals. Presence of struvite seed crystals or attachment surface reduces nucleation induction time and ion supersaturation requirements for struvite formation [10], [29].

Conclusions

While utilizing a RABR system for nutrient removal of municipal anaerobic digester effluent filtrate, struvite was observed in the microalgae biofilm. Struvite was quantified in RABR tank settled sludge three east/west growth development layers of microalgae biofilm. Component ion molar ratios of Ca, Mg, and P in RABR tank water favor both struvite and calcium phosphate precipitation, but the microalgae biofilm favors struvite likely due to pH regulation and struvite nucleation.

The highest struvite content was observed in the bottom layer of the east biofilm and could be correlated to the higher microalgae content in that layer. Shading from upper biofilm layers may reduce photoinhibition and increase microalgae biodiversity in bottom layer biofilm, which may explain differences in struvite content. Struvite appears directly correlated with microalgae in the biofilm matrix. Struvite does not seem to be directly correlated to TS, ash content, diatom content, biofilm development time, or sun-induced evaporation alone, but all may be factors.

More research is needed to determine the exact mechanism of struvite formation in microalgae biofilm matrix. Measuring the pH gradient through different biofilm layers and at the cellular interface within the biofilm matrix may elucidate struvite formation potential in different layers. Measuring zeta potential may also help define pH differences

between biofilm cells and trapped wastewater. Detailed species composition of mixed microalgae biofilm may determine if certain species are more correlated to struvite precipitation. To quantify struvite correlation with biofilm health, photosynthetic activity and chlorophyll concentration should be compared to relative struvite content. Optimization of struvite production could be evaluated through biofilm development times, PAR, and disk RPM. Multiple RABR systems connected in series or a synthetic wastewater experiment may clarify required molar concentrations of Mg:Ca:P, sludge, and TSS for struvite formation in mixed microalgae biofilm.

CHAPTER 2

STRUVITE PRECIPITATION TEST ON SETTLED ROTATING ALGAL BIOFILM REACTOR INFLUENT

Introduction

As stated in Chapter 1, the RABR appears to sequester struvite in the microalgae biofilm. Little struvite appears in the settled sludge, but calcium phosphate may be present according to Table 3. To better understand if pH is the primary driver in struvite formation within RABR microalgae biofilm, a jar test was performed on settled RABR influent at five distinct pH values.

If pH is the primary driver, struvite should precipitate in the jar test. However, influent component ion molar ratios of Mg, Ca, and P could allow for calcium phosphate precipitation [16]. Thus, the microalgae biofilm may provide conditions for the specific formation of struvite if calcium phosphate is the primary precipitate observed in the jar test. The microalgae biofilm may provide nucleation surfaces and a pH range favorable to struvite over calcium phosphate precipitation [10], [29]**.** The jar test eliminates influences of the microalgae biofilm and isolates the effect of pH on precipitate composition.

Materials and Methods

Fresh RABR influent was collected at CVWRF and brought to the USU Innovations Campus for the precipitation experiment. Influent settled for 1 hour and 900 mL of supernatant was collected in a 1000 mL beaker for each pH experiment. A Mettler-

Toledo FiveGo portable pH and conductivity probe was used to measure pH. The probe was calibrated before the experiment start and periodically throughout the experiment. The goal pH values for the experiment were 7.9, 8.0, 8.1, 8.2, and 8.3 to reflect the measure pH range for RABR water and biofilm (Table 2).

The native pH for the settled influent was 8.15. Each of the 5 samples was acidified to a baseline pH of 7.9 or below using 1 N sulfuric acid (H_2S0_4) before the precipitation test began. A Phipps & Bird Programmable JarTester was used to continually stir the samples at 3 RPM. Each solution was adjusted to the goal pH using 0.1 N NaOH with 15 minutes of mixing between each adjustment to ensure adequate time for pH stabilization. Over the course of the 15 to 18.5-hour precipitation experiment, pH was adjusted every 1-6 hours using 1 N H_2S0_4 and 0.1 N NaOH as necessary to maintain the goal pH. Precipitation time varied depending on how long it took to reach the goal pH or time between sample preparation.

After 15-18.5 hours of mixing, the samples were filtered using 0.7-micron GF/F Whatman glass microfiber filters (Cat. No. 1825-047). All containers and filtration equipment were rinsed with 1N H_2S0_4 then DI water to remove contaminants between samples. All filters were soaked in DI water for 6 hours to remove potential P contamination from the filters. Each sample required 2-3 filters due to filter clogging. After filtration, the filters were dried on the benchtop at room temperature for 2 hours then placed in a desiccator until weight was constant. Two and three-filter controls were prepared by soaking filters in DI water, drying on the benchtop, then placing in the desiccator. Filtrate was acidified using 1 N H_2S0_4 and stored at 4°C.

Filters from each sample were placed in 50-mL beakers, then 30 mL of 1N H_2S0_4 was added to each beaker to cover the filters. The filters were swirled for 2 minutes to dissolve phosphate precipitates. Particulates from the filter was observed in solution, so the solution was filtered again through treated, 0.7-micron glass microfiber filters.

The filters used to filter the dissolved precipitates were treated by filtering 50 mL of 1 N H_2S0_4 followed by 2 rinses of 100 mL DI water. Filtrate from each sample was collected in a 100 mL volumetric beaker. DI water was added up to 100 mL.

To measure struvite content in the precipitates, total nitrogen was measured for each sample using HACH Persulfate Digestion HR Test 'N Tube™ (Method 10072). Magnesium, calcium, and phosphate concentration was analyzed via ICP-MS.

Results and Discussion

Table 4 summarizes the pH values for each sample throughout the precipitation experiment. The pH tended to shift throughout the experiment likely because of the wastewater buffering capacity and CO_2 stripping effects from stirring [18], [30].

Table 4. Values for the pH precipitation test performed on settled RABR influent

Goal pH	H_2S0_4 Adjusted pH	NaOH adjusted Start pH	Maintained pH	Precipitation Time
7.9	7.90	7.90	7.9 ± 0.8	15 hours
8.0	7.69	8.00	8.0 ± 0.7	18.5 hours
8.1	7.86	8.09	8.1 ± 0.2	17 hours
8.2	7.69	8.18	8.2 ± 0.5	17 hours
8.3	7.71	8.29	8.3 ± 0.5	16 hours

Results from the Total N HACH kits were inconclusive. Measurements ranged from 0-1 mg/L NH_4-N. The lack of nitrogen in the samples could indicate there was no measurable struvite in the precipitates. Otherwise, extraction of N from the precipitates was unsuccessful. According to a HACH technical support representative, the levels of sulfuric acid in this experiment should not have caused interference with Method 10072 even without pH neutralization. White precipitates were observed in the jars after completion of the precipitation test, shown in Figure 14.

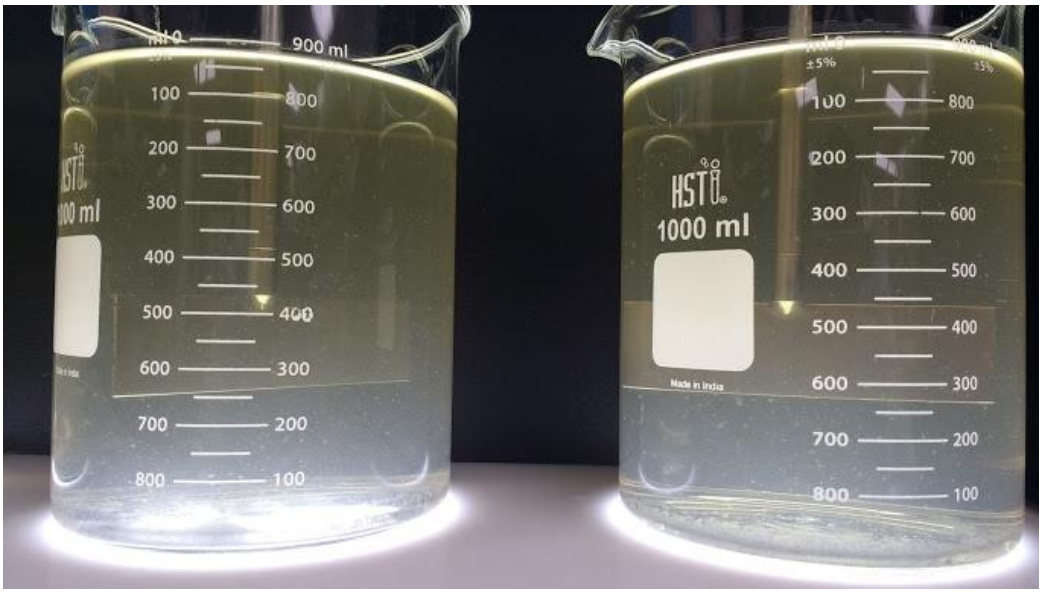

Figure 14. White precipitates visible in jars after completion of the precipitation test

Figure 15 shows molar concentration of Ca and Mg normalized to P. Magnesium and calcium phosphate precipitates are present. Calcium phosphate appears to dominate over magnesium phosphate. Component ion molar ratios of Mg and Ca are similar for the

precipitates from pH 7.9 to 8.2. The precipitates from pH 8.3 appear to contain less calcium phosphate than other pH values. Data and calculations for Figure 15 are in the Chapter 2 Appendix (Table 19).

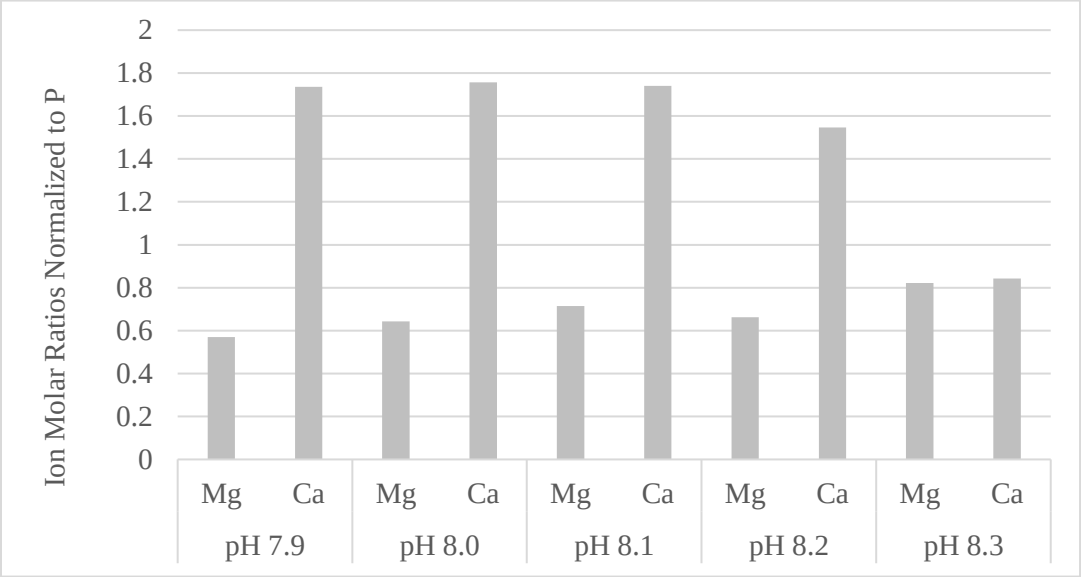

Figure 15. ICP-MS precipitation test results for precipitates dissolved in sulfuric acid. Molar concentration of Mg and Ca were normalized to the molar concentration of P.

J. Wang et al. (2005) performed a similar precipitation experiment using synthetic wastewater. However, they used HCl instead of H_2S0_4 and measured ammonium concentration using HACH HR, Test' N Tube Method 10031 instead of the HACH HR Total N Method 10072. J. Wang et al. (2005) did not specify if they pre-treated their filters, and they did not appear to filter their samples after precipitates were dissolved. J. Wang et al. (2005) successfully measured struvite content of precipitates using the

HACH ammonia method 10031.

Assuming the precipitates are not struvite, our experiment indicates that pH is not the main driving force for struvite formation in the RABR microalgae biofilm. Without nucleation sites provided by the biofilm, struvite is not the primary precipitate. From these results, it is unclear what precipitates were formed during the precipitation test. The Mg:Ca:P molar ratios in Figure 15 are like molar ratios calculated for RABR tank settled sludge in Table 3 that are dominated by Ca and P, but not struvite.

Conclusions

There are three possible conclusions from nitrogen content of precipitates formed during the precipitation test: 1) struvite content of the precipitates was negligible, 2) the HACH Persulfate Digestion HR Test 'N Tube™ (Method 10072) did not accurately measure nitrogen content of the precipitates, or 3) the method used for dissolving filtered precipitates was not appropriate. If struvite content of the precipitates is negligible, RABR microalgae biofilm provides nucleation sites or other favorable conditions essential for the specific formation of struvite in the RABR system. ICP-MS indicates that some struvite may be present in the precipitates, but calcium phosphate appears to dominate.

CHAPTER 3

CONTROL ROTATING ALGAL BIOFILM REACTORS FOR STRUVITE PRECIPITATION AT THE ALGAE PROCESSING AND PRODUCTS FACILITY

Introduction

After struvite was observed in the microalgae biofilm at the CVWRF RABR, it was hypothesized biofilm-bound struvite was the result of breakthrough sludge trapped in the biofilm. To test this hypothesis, a controlled experiment was set up at the Microalgae Processing and Products Facility (APP) at the USU Innovations Campus in Logan, UT. Two smaller-scale RABRs were built outdoors in the same east/west orientation as the pilot-scale RABR at CVWRF. Because the two APP RABRs were offsite of CVWRF, the two APP RABRs were run in batch instead of continuous-flow like the CVWRF RABR. Shade cloth was used on the APP RABRs to prevent photoinhibition. The influent source and inoculum were the same for the APP RABRs and CVWRF RABR.

Biofilm health was evaluated to test the alternative hypothesis that struvite is correlated to a healthier microalgae biofilm matrix. A healthy biofilm will have biodiversity dominated by microalgae and the biomass will be mostly green in color. If struvite does not form in the APP RABR microalgae biofilm, sludge entrapment and microalgae health are not the primary drivers in struvite formation. The continuous supply of wastewater high in Mg, N, and P may also be necessary for struvite formation in the RABR microalgae biofilm.

Materials and Methods

APP RABR Construction

RABR disks were constructed from 1 in. thick polystyrene insulation hard foam cut to approximately 23 in. diameter. A 3/8 in. hole was drilled in the center of each disk. A 1/2 in. hole was drilled in the center of 2 in. x 4 in. timber mending plates (Figure 16a) and a 5/8 in. shaft collar was glued to the mending plate using FuzeIt® (Figure 16b). Two mending plates were installed per disk and sandwiched the center hole of the polystyrene disk. The disks were mounted onto a 5/8 in. stainless steel rod, shown in Figure 16b. Each rod had 4 disks mounted to it. The surface of each disk was gouged in a random pattern using a screw to provide seeding sites for inoculum.

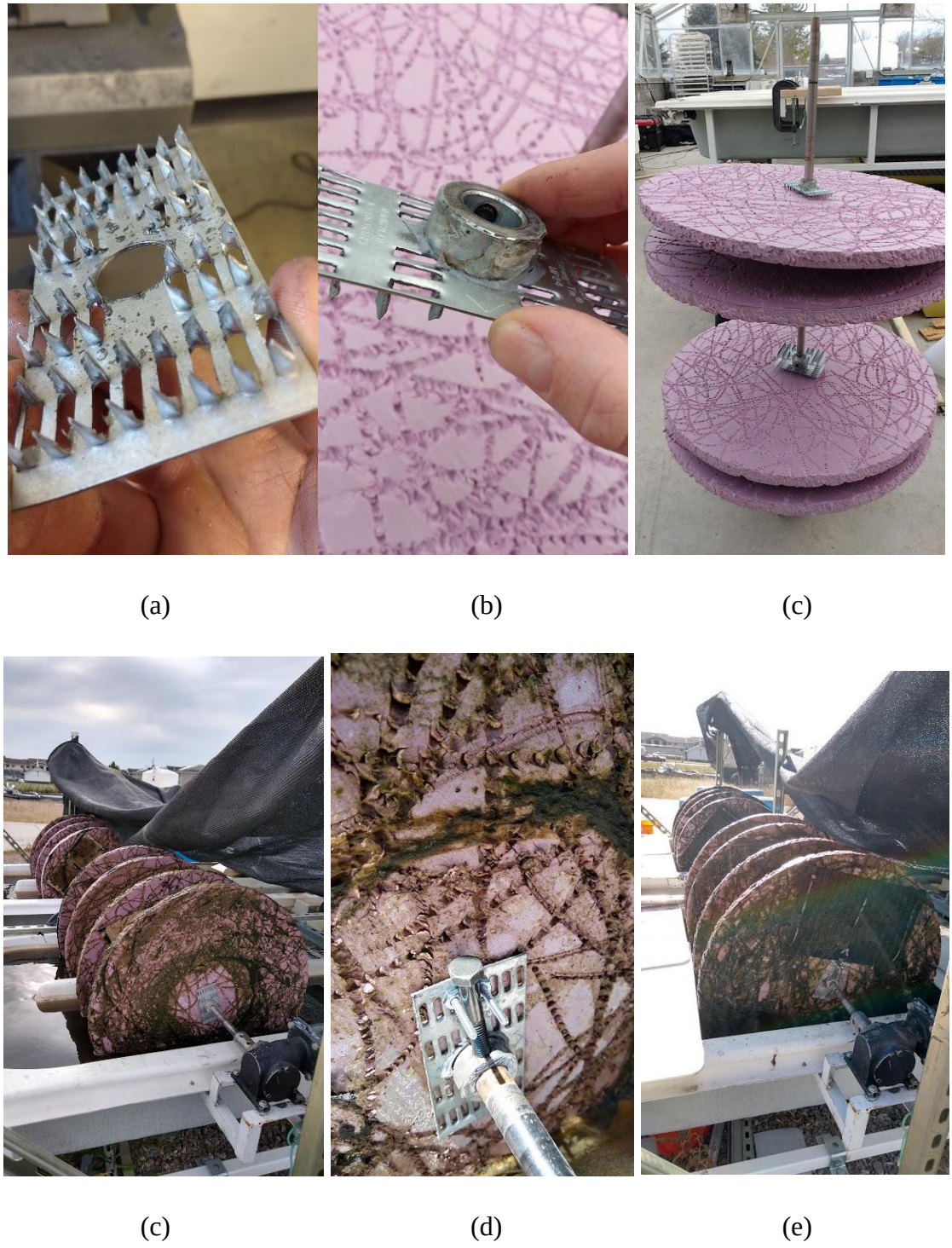

(a) (b) (c)

(c) (d) (e)

Figure 16. Construction and layout for APP RABRs

Shade cloth was installed to protect the microalgae biofilm from direct sunlight. The two disk rods were joined together and rotated using one motor (Figure 16c). The motors were Leeson Permanent Magnet gear motors (Model CM34D25NZ10C) with Leeson Speedmaster Washgaurd adjustable speed DC motor control panel. The motor was mounted to a 110-gallon fiberglass raceway such that four disks spanned one raceway and the other four disks spanned another raceway (Figure 16c). Paddles were mounted to another motor and installed in the same configuration centered in the raceways to mix the growth media.

The FuzeIt® initially used to glue the shaft collars to the timber mending plate did not hold. Bolts and machine screws successfully fastened the disks to the rods using the configuration shown in Figure 16d.

Solid white, high-density polyethylene (HDPE) panels were used to cover open water spaces on the raceways to block sunlight and prevent unwanted suspended growth within the raceways (Figure 16e). To improve microalgae biofilm productivity, durable carpet was cut into 12 in. x 7.5 in. rectangles. One rectangle was fastened to one side of each disk (Figure 16e). The carpet (Multi Home MT1001734) was 80% polyester and 20% polypropylene with a 100% gel backing.

Like the CVWRF RABR, every side of every APP RABR disk was inoculated with biofilm harvested from the CVWRF trickling filters. The west RABR, called RABR 1, contained CVWRF RABR settled influent supernatant. The east RABR, called RABR 2, contained CVWRF RABR settled influent supernatant with the settled sludge added

back into the water. RABR 1 was the control that contained no sludge and RABR 2 was the control that contained sludge. To maintain consistent water volume, tap water was added to the raceways as water evaporated. The APP RABRs operated from July 10, 2019 to August 29, 2019.

APP RABR Water and Biofilm pH

Water and biofilm pH were measured using a Mettler-Toledo FiveGo portable pH and conductivity probe, calibrated before every use. Biofilm pH was measured by inserting the probe into the biofilm soon after it emerged from the water. The sensing probe was fully submerged in the biofilm and allowed to calibrate for 1 minute. Water pH was measured intermittently from July 10 to August 29, 2018. Water was changed every 2-3 weeks with fresh CVWRF RABR settled influent supernatant to replenish Mg, N, and P for the batch reaction. The settled sludge from the influent was added to RABR 2 every time water was changed. ANOVA was used to determine statistical significance between pH values.

APP RABR Water Nutrient Analysis

Dissolved N, P, and Mg in RABR 1 and RABR 2 water was measured over the course of 16 days from July 24 to August 8, 2019. Water was not changed in this time period, but tap water was added as needed to maintain constant volume.

Each water sample was filtered through a treated 0.7-micron GF/F Whatman glass microfiber filter (Cat. No. 1825-047). Filters were treated by soaking in DI water for 24 hours according to Standard Methods, 21st Edition (2005) to remove excess P from the filter [14].

Total N was measured using HACH Test N' Tube High Range Total Nitrogen (Persulfate) reagent set 2714045 with Total Nitrogen Acid Solution reagent set 2672145. Total P was measured using HACH Test N' Tube High Range Total Phosphate (Molybdovanadate) reagent set 2767245. A HACH DRB 200 (SN: 13040C0073) was used for the heat reactions. Absorbance was measured using a HACH DR 2700 Portable Spectrophotometer (SN: 1241813). The HACH Hardness, Total and Calcium (EDTA titration) Test Kit (Cat. No. 145701) was used to measure Mg concentration, calculated by subtracting Ca hardness from total hardness.

Light Microscopy and SEM/EDS Analysis of Microalgae Biofilm

RABR 1 and RABR 2 biofilm samples were analyzed using a light microscope (Leica DM 750) and high-resolution digital camera (Leica ICC 50) to look for struvite crystals within the microalgae biofilm matrix. SEM/EDS was performed by the Utah State University Office of Research, Microscopy Core Institute to confirm presence or absence of struvite crystals in the RABR 1 and RABR 2 microalgae biofilms.

Results and Discussion

APP RABR Water and Biofilm pH

Figure 17 shows significant fluctuation between pH 7 and 8.5 over time in both RABRs. It is unclear what caused the pH fluctuation. There was no statistical difference between water and biofilm pH for both RABR 1 and RABR 2. Biofilm was expected to have higher pH than water due to photosynthesis in the biofilm. Data and calculations for Figure 17 are in the Chapter 3 Appendix (Tables 20-21) including standard deviation.

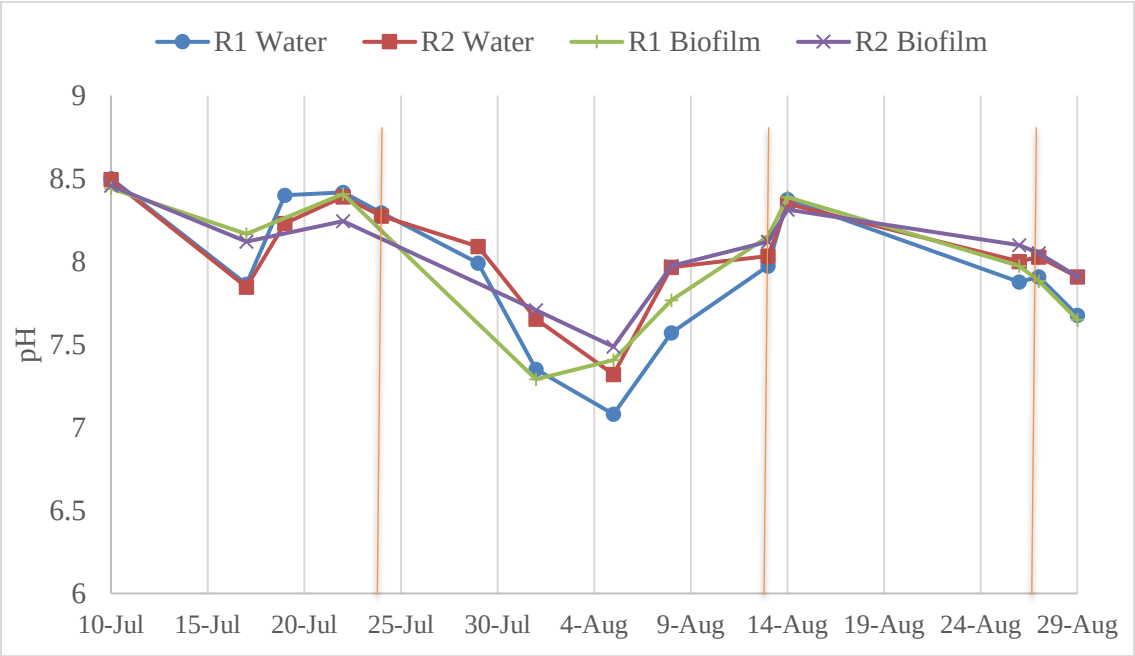

Figure 17. APP RABR 1 (R1) and RABR 2 (R2) biofilm and water pH comparison over time. Orange bars indicate when water was changed.

APP RABR pH data from March 7 to July 3 was omitted from Figure 17 because suspended growth significantly increased pH values up to approximately pH 10. Even with the significant increase in water pH, biofilm pH followed the same trend as water pH. RABR water pH seems to be the main factor in biofilm pH, or the main influence on the pH probe reading.

Nitrogen, Phosphorus, and Magnesium Concentration of RABR Water

Figure 18 shows that N, P, and Mg concentration between RABR 1 and RABR 2 are not significantly different. The N and P trends are inconclusive because there is no significant change over time nor a consistent trend. The increase in Mg could be from tap

water added to the system. Despite visible microalgae biofilm growth, N and P concentration in the wastewater does not significantly change. Data and calculations for Figure 18 are in the Chapter 3 Appendix (Table 22).

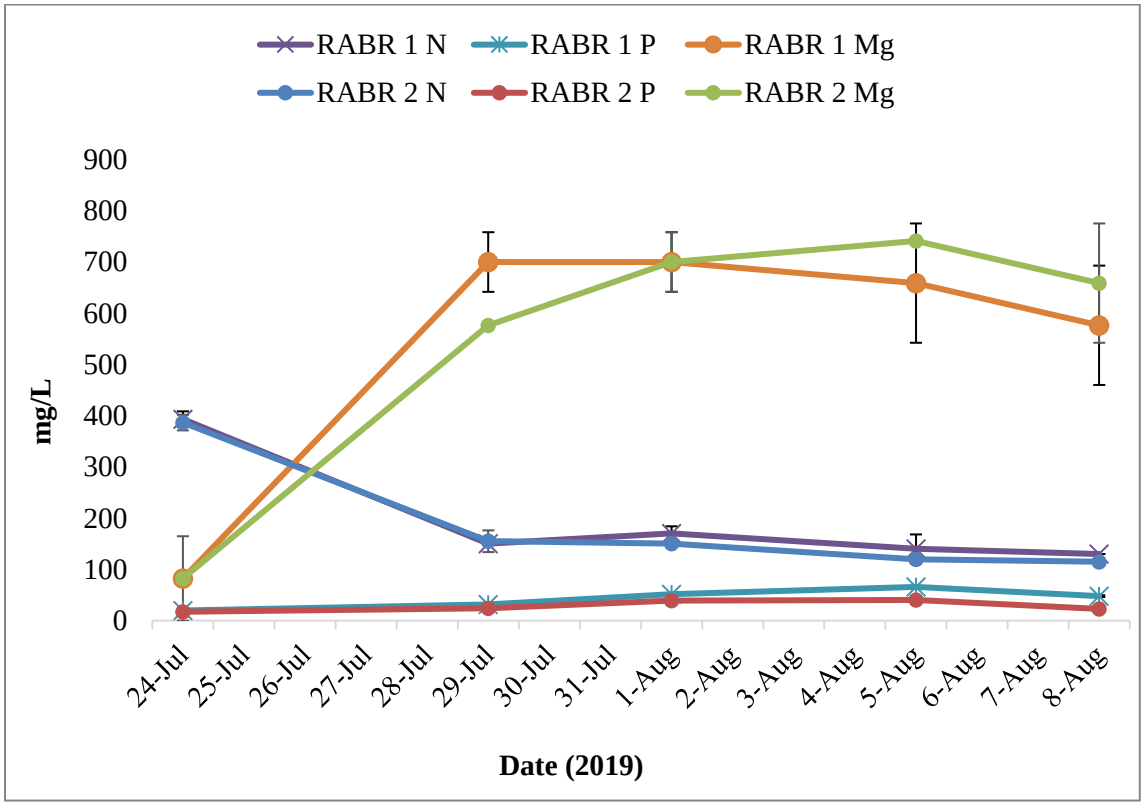

Figure 18. Nitrogen (N), phosphorus (P), and magnesium (Mg) concentration in filtered RABR water over the 16-day period between July 24 and August 8, 2019 shows no significant differences nor consistent trends between RABR 1 and RABR 2. The data points are averaged values between duplicate samples and error bars indicate standard deviation.

Light Microscopy and SEM/EDS Analysis of Microalgae Biofilm

Light microscopy revealed no struvite crystals in the RABR 1 and RABR 2

microalgae biofilms. SEM/EDS confirmed this result. No crystals were found within the either microalgae biofilm despite apparent biofilm health, shown in Figure 19.

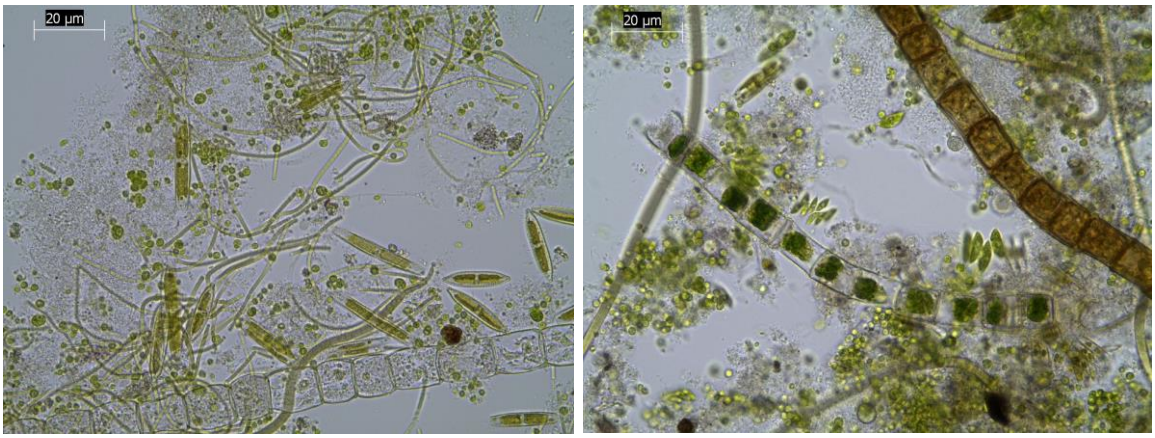

(a) **(b)**

Figure 19. (a) RABR 1 microalgae biofilm at 40X magnification and **(b)** RABR 2 microalgae biofilm at 40X magnification show a healthy bioconsortia like the east bottom layer of the CVWRF RABR.

The shade cloth at the APP RABRs contributed to a healthy bioconsortia within both APP RABR microalgae biofilms, further indicating that RABR microalgae biofilm appears healthier when not exposed to excessive direct sunlight. A healthy biofilm is not the only requirement for struvite precipitation, otherwise struvite would have appeared in the APP RABR microalgae biofilms.

The struvite in the CVWRF RABR is not the result of sludge buildup alone. If sludge buildup were the cause of struvite in the biofilm, RABR 2 would most likely contain struvite. Struvite precipitation within the microalgae biofilm matrix at CVWRF

cannot be attributed to biofilm health alone nor sludge buildup alone.

The CVWRF RABR has continuous-flow anaerobic digester filtrate with high N, P, and Mg. The batch setup at the APP may not have had a continuously high enough influent of struvite constituents to supersaturate like in the CVWRF RABR. A continuous flow of supersaturated wastewater may be required for struvite precipitation within RABR microalgae biofilm matrix.

Conclusions

The APP RABR control experiment was unsuccessful at producing struvite in the microalgae biofilm matrix. The APP RABR biofilms appeared just as healthy or healthier than the healthiest layer at the CVWRF RABR, but still no struvite was present. Sludge entrapment is not the primary source of struvite present in the CVWRF biofilm because there was no struvite in the sludge control, APP RABR 2. Sludge entrapment may still play a role at the CVWRF RABR by providing small seed crystals, but the sludge control experiment was inconclusive. The continuous flow of anaerobic digester pressate supersaturated with N, P, and Mg is likely key to struvite formation in the CVWRF RABR microalgae biofilm matrix. The APP RABRs used the same anaerobic digester pressate but were run in batch instead of continuous-flow. Because struvite was not found in the APP RABR microalgae biofilm matrices, continuous-flow may be required for struvite formation in RABR microalgae biofilm.

CHAPTER 4

ENGINEERING SIGNIFICANCE AND SUGGESTED FUTURE STUDIES

Struvite precipitation in RABR microalgae biofilm matrix could provide an alternative to other methods of struvite precipitation such as CO_2 stripping. Biofilm struvite precipitation does not require costly CO_2 stripping to increase water pH and does not require the addition of carbon like many biological P removal processes. The RABR system removes N and P through biofilm metabolic activity and struvite precipitation, which is efficient, sustainable, and generates a marketable fertilizer bioproduct.

For RABR-mediated struvite precipitation to be implemented at a large scale, more research is needed to understand the influences on struvite precipitation in the microalgae biofilm matrix. Struvite precipitation at the CVWRF RABR is influenced by east/west sun orientation, harvesting interval, sun exposure, pH, temperature, and a continuous flow of wastewater supersaturated with N, P, and Mg. The magnitude and optimal range for those influences should be investigated.

A detailed species composition of microalgae biofilm known to contain struvite may help determine which microalgae species are correlated to struvite precipitation. Photosynthetic activity and chlorophyll content of struvite-containing biofilm should be compated to struvite content within the biofilm to understand how biofilm health impacts struvite content. Biofilm growth and struvite precipitation could be optimized by adjusting PAR, biofilm development times, and disk RPM. Multiple pilot-scale RABRs could be connected in series to better understand continuous-flow N, P, and Mg concentration requirements for struvite precipitation in RABR microalgae biofilm. A tank

series would also allow sludge to settle between tanks to understand the influence of sludge and TSS. A synthetic wastewater experiment could determine what wastewater constituents are necessary and the concentration of constituents required for struvite formation within a microalgae biofilm.

REFERENCES

[1] H. Melcer and T. Lindley, “CVWRF Side Stream Phosphorus Removal Analysis, v.4. Draft Memorandum Prepared for Central Valley Water Reclamation Facility.” Unpublished Draft Memorandum Prepared by Brown and Caldwell, Midvale, 2019.

[2] K. M. Waddell *et al.*, “Water Quality in the Great Salt Lake Basins, Utah, Idaho, and Wyoming, 1998-2001,” 2003.

[3] A. H. Cabije, R. C. Agapay, and M. V Tampus, “Carbon-nitrogen-phosphorus removal and biofilm growth characteristics in an integrated wastewater treatment system involving a rotating biological contactor,” *Asia-Pacific J. Chem. Eng.*, vol. 4, no. 5, pp. 735–743, Sep. 2009.

[4] L. Delgadillo-Mirquez, F. Lopes, B. Taidi, and D. Pareau, “Nitrogen and phosphate removal from wastewater with a mixed microalgae and bacteria culture,” *Biotechnol. Reports*, vol. 11, pp. 18–26, Sep. 2016.

[5] X.-D. Hao, C.-C. Wang, L. Lan, and M. C. M. van Loosdrecht, “A quantitative method analyzing the content of struvite in phosphate-based precipitates,” in *International Conference on Nutrient Recovery From Wastewater Streams*, Vancouver: IWA Publishing, 2009, pp. 79–88.

[6] R. W. Sterner and J. J. Elser, *Ecological Stoichiometry: The Biology of Elements from Molecules to the Bioshphere*, 1st ed. Princeton: Princeton University Press, 2002.

[7] Peterson, B. L. "Development and optimization of a produced water, biofilm based

microalgae cultivation system for biocrude conversion using hydrothermal liquefaction." *All Graduate Theses and Dissertations.* Utah State University. 2018. https://digitalcommons.usu.edu/etd/7237/

[8] A. Hodges, Z. Fica, J. Wanlass, J. VanDarlin, and R. Sims, "Nutrient and suspended solids removal from petrochemical wastewater via microalgal biofilm cultivation," *Chemosphere*, vol. 174, pp. 46–48, 2017.

[9] L. B. Christenson and R. C. Sims, "Rotating algal biofilm reactor and spool harvester for wastewater treatment with biofuels by-products," *Biotechnol. Bioeng.*, vol. 109, no. 7, pp. 1674–1684, Jul. 2012.

[10] J. D. Doyle and S. A. Parsons, "Struvite formation, control and recovery," *Water Res.*, vol. 36, no. 16, pp. 3925–3940, Sep. 2002.

[11] C. Wang, X. Yu, H. Lv, and J. Yang, "Nitrogen and phosphorus removal from municipal wastewater by the green alga Chlorella sp.," *J. Environ. Biol.*, vol. 34, no. SUPPL.2, pp. 421–425, Apr. 2013.

[12] M. Szymanska, E. Szara, A. Was, T. Sosulski, G. W. P. Van Pruissen, and R. L. Cornelissen, "Struvite—an innovative fertilizer from anaerobic digestate produced in a bio-refinery," *Energies*, vol. 12, no. 2, pp. 1–9, 2019.

[13] M. Gross, D. Jarboe, and Z. Wen, "Biofilm-based algal cultivation systems," *Appl. Microbiol. Biotechnol.*, vol. 99, no. 14, pp. 5781–5789, Jul. 2015.

[14] American Public Health Association, American Water Works Association, and Water Environment Federation, *Standard methods for the examination of water and wastewater*, 21st ed. Washington, DC: American Public Health Association,

2005.

[15] J.-K. Wang and M. Seibert, “Prospects for commercial production of diatoms.,” *Biotechnol. Biofuels*, vol. 10, p. 16, 2017.

[16] J. Wang, J. G. Burken, X. (Jackie) Zhang, and R. Surampalli, “Engineered Struvite Precipitation: Impacts of Component-Ion Molar Ratios and pH,” *J. Environ. Eng.*, vol. 131, no. 10, pp. 1433–1440, Oct. 2005.

[17] K. S. Le Corre, E. Valsami-Jones, P. Hobbs, and S. A. Parsons, “Phosphorus Recovery from Wastewater by Struvite Crystallization: A Review,” *Crit. Rev. Environ. Sci. Technol.*, vol. 39, no. 6, pp. 433–477, Jun. 2009.

[18] B. Bergmans, “Struvite recovery from digested sludge At WWTP West,” Delft University of Technology, 2011.

[19] D. Radev, G. Peeva, and V. Nenov, “pH Control during the Struvite Precipitation Process of Wastewaters,” *Wastewaters. J. Water Resour. Prot.*, vol. 7, pp. 1399–1408, 2015.

[20] T. Esemen, W. Rand, T. Dockhorn, and N. Dichtl, “Increasing cost efficiency of struvite precipitation by using alternative precipitants and P-remobilization from sewage sludge,” in *International Conference on Nutrient Recovery From Wastewater Streams*, K. Ashley, D. Mavinic, and F. Koch, Eds. Vancouver: IWA Publishing, 2009, pp. 269–331.

[21] Y.-H. Song *et al.*, “Nutrients removal and recovery from anaerobically digested swine wastewater by struvite crystallization without chemical additions,” *J. Hazard. Mater.*, vol. 190, no. 1–3, pp. 140–149, Jun. 2011.

[22] R. J. Craggs, J. P. Sukias, C. T. Tanner, and R. J. Davies-Colley, “Advanced pond system for dairy-farm effluent treatment,” *New Zeal. J. Agric. Res.*, vol. 47, no. 449, pp. 449–460, 2004.

[23] J. B. K. Park, R. J. Craggs, and A. N. Shilton, “Wastewater treatment high rate algal ponds for biofuel production,” *Bioresour. Technol.*, vol. 102, no. 1, pp. 35–42, Jan. 2011.

[24] W. K. Dodds, B. J. F. Biggs, and R. L. Lowe, “Photosynthesis-irradiance patterns in benthic microalgae: variations as a function of assemblage thickness and community structure,” *J. Phycol.*, vol. 35, no. 1, pp. 42–53, Feb. 1999.

[25] S. Roberts, S. Sabater, and J. Beardall, “Benthic microalgal colonization in streams of differing riparian cover and light availability,” *J. Phycol.*, vol. 40, no. 6, pp. 1004–1012, Dec. 2004.

[26] C. Sorokin and R. W. Krauss, “The Effects of Light Intensity on the Growth Rates of Green Algae.,” *Plant Physiol.*, vol. 33, no. 2, pp. 109–13, Mar. 1958.

[27] J. Komárek and J. R. Johansen, “Filamentous Cyanobacteria,” in *Freshwater Algae of North America*, 2nd ed., J. D. Wehr, R. G. Sheath, and J. P. Kociolek, Eds. Academic Press, 2015, pp. 135–235.

[28] M. Gross, “The mysteries of the diatoms,” *Curr. Biol.*, vol. 22, no. 15, pp. R581–R585, Aug. 2012.

[29] S. Agrawal, J. S. Guest, and R. D. Cusick, “Elucidating the impacts of initial supersaturation and seed crystal loading on struvite precipitation kinetics, fines production, and crystal growth,” *Water Res.*, vol. 132, pp. 252–259, Apr. 2018.

[30] L. Lijklema, “Factors affecting pH change in alkaline wastewater treatment -- I,” *Water Res.*, vol. 3, pp. 913–930, 1969.

[31] K. Hori *et al.*, “Klebsormidium flaccidum genome reveals primary factors for plant terrestrial adaptation,” *Nat. Commun.*, vol. 5, no. 1, p. 3978, Sep. 2014.

APPENDICES

Chapter 1 Appendix

Trickling Filter Microalgae used for RABR Biofilm Inoculum

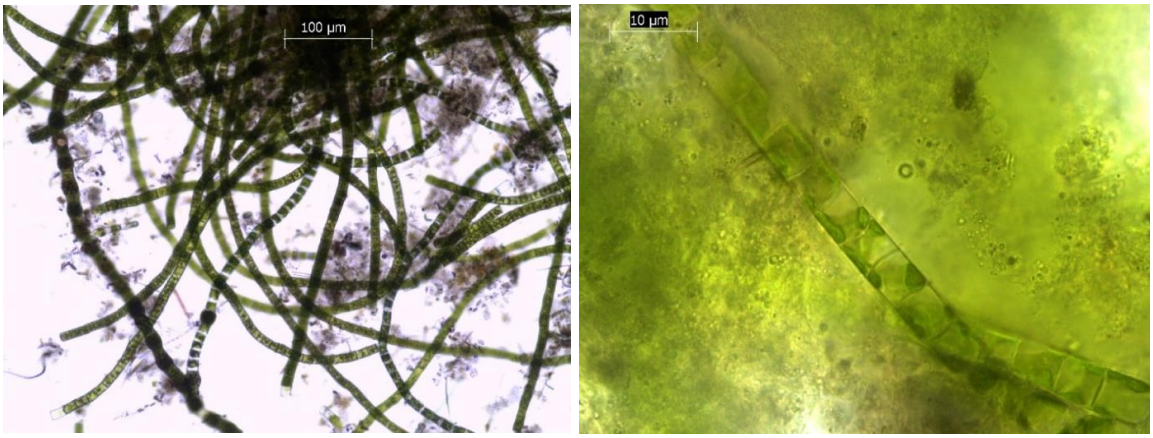

(a) **(b)**

(c)

Figure 20. Trickling filter algae that was used as the inoculum for the CVWRF RABR magnified at 10X **(a)**, 100X **(b)**, and 40X **(c)**. Trickling filter biofilm consisted *Chlorella*, *Nitzschia*, *Navicula*, *Oscillatoria*, *Ulothrix*, and *Klebsormidium*, shown in appendix [14], [31].

Data and ANOVA for Table 2

Table 5. Temperature and pH data of CVWRF RABR tank water and microalgae biofilm

Date (2019)	Sample	pH	mV	Temp (C)
28-Jun	RABR Water	8	-52	23.9
		7.68	-34	23.8
		7.55	-27	23.9
	Biofilm	7.96	-51	29.8
		7.97	-52	30.8
		7.96	-50	26.1
26-Jul	RABR Water	7.55	-27	27.9
		7.71	-36	26.4
		7.98	-51	25.7
	Biofilm	8.06	-55	22.8
		8.06	-55	22.6
		8.04	-54	23
9-Aug	RABR Water	7.5	-27	27.7
		7.3	-16	26.5
		7.23	-12	27.1
		7.92	-51	28.4
	Biofilm	8.02	-57	28.2
		8.02	-57	28.5
		8.02	-57	28.8
		8	-56	28.4
16-Aug	RABR Water	8.02	-55	25.6
		8.06	-57	25.6
		8.06	-57	25.6
		8.07	-57	25.5
	Biofilm	7.98	-53	27
		8.04	-56	26.6
		8.05	-56	26.3
		8.01	-54	27.2

23-Aug	RABR Water	8.01	-53	26.3
		8.01	-53	26.3
		8.01	-53	26.4
	Biofilm	8.01	-53	26.1
		8.05	-55	24.4
		8.04	-55	24.1
		8.03	-54	24.6

Table 6. Average and standard deviation for CVWRF RABR microalgae biofilm and water pH calculated from data in Table 5.

	pH Average		pH SD	
Date	Water	Biofilm	Water	Biofilm
28-Jun	7.743333	7.963333	-0.23159	0.005774
26-Jul	7.746667	8.053333	0.217332	0.011547
9-Aug	7.4875	8.015	0.310202	0.01
16-Aug	8.0525	8.02	0.022174	0.031623
23-Aug	8.01	8.0325	0	0.017078

Table 7. ANOVA: two-factor without replication for statistical comparison of CVWRF RABR microalgae biofilm and water pH using the data in Table 5. ANOVA was calculated using Microsoft Excel data analysis and shows the p-value is >0.05. Thus, biofilm and tank water pH are not significantly different

SUMMARY	*Count*	*Sum*	*Average*	*Variance*
Row 1	2	15.70667	7.853333	0.0242
Row 2	2	15.8	7.9	0.047022
Row 3	2	15.5025	7.75125	0.139128
Row 4	2	16.0725	8.03625	0.000528
Row 5	2	16.0425	8.02125	0.000253
Column 1	5	39.04	7.808	0.052812
Column 2	5	40.08417	8.016833	0.001113

ANOVA

Source of Variation	*SS*	*df*	*MS*	*F*	*P-value*	*F crit*
Rows	0.113598	4	0.0284	1.112582	0.460069	4.10725
Columns	0.109028	1	0.109028	4.271302	0.10763	4.544771
Error	0.102103	4	0.025526			
Total	0.32473	9				

Data and Calculations for Table 3

Table 8. Data from ICP-MS used for Table 3 calculations

			24 Mg [He]	31 P [He]	44 Ca [He]
Sample Name	g of powder added to 10 mL sulfuric acid	kg sample / L	Conc. [mg/l]	Conc. [mg/l]	Conc. [mg/l]
CVWRF RABR Influent	N/A	N/A	46.56	11.31	76.61
Influent	N/A	N/A	44.16	13.27	90.02
Influent	N/A	N/A	43.31	12.59	87.93
CVWRF RABR Effluent	N/A	N/A	47.02	11.62	76.73
Effluent	N/A	N/A	41.85	12.42	82.72
Effluent	N/A	N/A	44.01	12.94	85.11
Trickling #2	0.2963	0.02963	204.71	297.60	762.14
Trickling #3	0.2371	0.02371	185.03	258.06	746.52
Biofilm #1	0.7586	0.07586	10044.82	13923.97	716.16
Biofilm #2	0.4275	0.04275	5555.50	7432.15	1560.07
Biofilm #3	0.1927	0.01927	1923.08	2840.92	548.88
Sludge #1	0.1564	0.01564	160.23	395.48	765.61
sludge #4	0.1535	0.01535	158.74	358.24	693.59
sludge #5	0.1967	0.01967	174.80	434.77	740.70

Table 9. Calculations for molar content of Mg, Ca, and P for CVWRF trickling filter microalgae biofilm, RABR biofilm, and RABR tank settled sludge using ICP-MS data in Table 8.

Sample	g Mg / kg Sample	g P / kg Sample	g Ca / kg Sample	mol Mg / kg Sample	mol P / kg Sample	mol Ca / kg Sample	Mg/P	Mg:P (Molar)	Ca/P	Ca:P (Molar)	Ca:Mg:P (Molar)	Mg/Ca	Mg:Ca (Molar)
Trickling Ave	7.36	10.46	28.60	0.30	0.34	0.71	0.90	0.90:1	2.11	2.1:1	2.1:0.9:1	0.42	0.42:1
Trickling SD	0.63	0.59	4.08	0.03	0.02	0.10	-	-	-	-	-	-	-
Trickling Coefficient of Variation	0.09	0.06	0.14	0.09	0.06	0.14	-	-	-	-	-	-	-
Biofilm Ave	120.72	168.28	24.81	4.11	3.97	0.62	1.03	1.03:1	0.16	0.16:1	0.2:1.0:1	6.63	6.6:1
Biofilm SD	18.16	18.70	13.90	N/A	N/A	0.35	-	-	-	-	-	-	-
Biofilm Coefficient of Variation	0.15	0.11	0.56	N/A	N/A	0.56	-	-	-	-	-	-	-
Sludge Ave	9.82	23.58	43.93	0.40	0.76	1.10	0.53	0.53:1	1.44	1.4:1	1.4:0.5:1	0.37	0.37:1
Sludge SD	0.81	1.60	5.75	0.03	0.05	0.14	-	-	-	-	-	-	-
Sludge Coefficient of Variation	0.08	0.07	0.13	0.08	0.07	0.13	-	-	-	-	-	-	-
Biofilm - Trickling	113.36	157.81	-3.80	3.80	3.63	-0.09	-	-	-	-	-	-	-
Biofilm - Trickling - Sludge	103.54	134.24	-47.73	3.40	2.87	-1.19	-	-	-	-	-	-	-

Continued…

Table 9 continued…

Sample	g Mg / kg Sample	g P / kg Sample	g Ca / kg Sample	mol Mg / kg Sample	mol P / kg Sample	mol Ca / kg Sample	Mg/P	Mg:P (Molar)	Ca/P	Ca:P (Molar)	Ca:Mg:P (Molar)	Mg/Ca	Mg:Ca (Molar)
% diff biofilm	14.23	20.23	292.41	17.22	27.67	292.41	-	-	-	-	-	-	-
% increase in biofilm (acct for inoculum)	93.91	93.78	-15.31	92.63	91.49	-15.31	-	-	-	-	-	-	-
% increase in biofilm (acct for inoculum and sludge)	85.77	79.77	-192.41	82.78	72.33	-192.41	-	-	-	-	-	-	-

Table 10. Statistics for influent and effluent Mg, P, and Ca concentration from Table 8

	24 Mg [He]	31 P [He]	44 Ca [He]
Sample	Conc. [mg/l]	Conc. [mg/l]	Conc. [mg/l]
Inf Ave	44.68	12.39	84.85
Inf SD	1.68	0.99	7.21
Inf Coefficient of Variation	0.04	0.08	0.08
Eff Ave	44.29	12.33	81.52
Eff SD	2.60	0.67	4.32
Eff Coefficient of Variation	0.06	0.05	0.05

Data, Calculations, and ANOVA for Figure 1

Table 11. Calculations for struvite content in TS and Ash using Data obtained from Total N HACH kits.

			Replicates		Replicates		Replicates	
Sample	Ash (g)	Ash (mg/L)	NH3-N (mg/L)	NH3-N (mg/L)	mg NH3 / mg Ash	mg NH3 / mg Ash	wt % NH3 of Ash	wt % NH3 of Ash
Trick Filt	3.2E-01	3.2E+03	2.0E+00	1.0E+00	6.2E-04	3.1E-04	6.2E-02	3.1E-02
Sludge	9.9E-02	9.9E+02	4.0E+00	2.0E+00	4.0E-03	2.0E-03	4.0E-01	2.0E-01
SE Poly Bot	3.3E-01	3.3E+03	2.4E+01	2.2E+01	7.3E-03	6.7E-03	7.3E-01	6.7E-01
SE Poly 1-wk	2.5E-01	2.5E+03	3.0E+00	6.0E+00	1.2E-03	2.4E-03	1.2E-01	2.4E-01
SE Poly Old	1.2E-01	1.2E+03	2.0E+00	2.0E+00	1.6E-03	1.6E-03	1.6E-01	1.6E-01
SW Poly Bot	4.4E-01	4.4E+03	1.9E+01	1.9E+01	4.4E-03	4.4E-03	4.4E-01	4.4E-01
SW Poly 1-wk	7.1E-01	7.1E+03	3.5E+01	3.6E+01	4.9E-03	5.1E-03	4.9E-01	5.1E-01
SW Poly Old	2.0E-01	2.0E+03	4.0E+00	4.0E+00	2.0E-03	2.0E-03	2.0E-01	2.0E-01

Continued…

Table 11 Continued…

	Replicates			Replicates									
Sample	mg struvite / mg Ash	mg struvite / mg Ash	mg Ash / mg TS	mg Struvite / mg TS	mg Struvite / mg TS	mg Struvite / mg TS AVE + SD	mg Struvite / mg TS AVE - SD	% Struvite in TS	% Struvite in TS	% Struvite / mg TS AVE	% Struvite / mg TS SD	% Struvite / mg TS AVE + SD	% Struvite / mg TS AVE - SD
Trick Filt	8.9E-03	4.5E-03	2.4E-01	2.2E-03	1.1E-03	2.4E-03	8.6E-04	2.2E-01	1.1E-01	1.6E-01	7.7E-02	2.4E-01	8.6E-02
Sludge	5.8E-02	2.9E-02	2.2E-01	1.3E-02	6.4E-03	1.4E-02	5.1E-03	1.3E+00	6.4E-01	9.6E-01	4.5E-01	1.4E+00	5.1E-01
SE Poly Bot	1.0E-01	9.6E-02	5.0E-01	5.2E-02	4.8E-02	5.3E-02	4.7E-02	5.2E+00	4.8E+00	5.0E+00	3.1E-01	5.3E+00	4.7E+00
SE Poly 1-wk	1.7E-02	3.4E-02	4.2E-01	7.2E-03	1.4E-02	1.6E-02	5.7E-03	7.2E-01	1.4E+00	1.1E+00	5.1E-01	1.6E+00	5.7E-01
SE Poly Old	2.3E-02	2.3E-02	5.2E-01	1.2E-02	1.2E-02	1.2E-02	1.2E-02	1.2E+00	1.2E+00	1.2E+00	0.0E+00	1.2E+00	1.2E+00
SW Poly Bot	6.3E-02	6.3E-02	6.8E-01	4.2E-02	4.2E-02	4.2E-02	4.2E-02	4.2E+00	4.2E+00	4.2E+00	0.0E+00	4.2E+00	4.2E+00
SW Poly 1-wk	7.1E-02	7.3E-02	5.6E-01	4.0E-02	4.1E-02	4.1E-02	4.0E-02	4.0E+00	4.1E+00	4.0E+00	8.1E-02	4.1E+00	4.0E+00
SW Poly Old	2.9E-02	2.9E-02	5.1E-01	1.5E-02	1.5E-02	1.5E-02	1.5E-02	1.5E+00	1.5E+00	1.5E+00	0.0E+00	1.5E+00	1.5E+00

Table 12. ANOVA: Single factor for statistical significance of struvite content in TS between CVWRF RABR microalgae biofilm layers. A p-value <0.05 is considered significantly different. Significantly different p-values are highlighted yellow while insignificant differences are highlighted red.

West 1-wk vs Bot

SUMMARY

Groups	*Count*	*Sum*	*Average*	*Variance*
Column 1	2	8.496962	4.248481	0
Column 2	2	8.096405	4.048202	0.006502

ANOVA

Source of Variation	*SS*	*df*	*MS*	*F*	*P-value*	*F crit*
Between Groups	0.040111	1	0.040111	12.33845	0.072361	18.51282
Within Groups	0.006502	2	0.003251			
Total	0.046613	3				

East 1-wk vs Old

SUMMARY

Groups	*Count*	*Sum*	*Average*	*Variance*
Column 1	2	2.169331	1.084665	0.261444
Column 2	2	2.427897	1.213948	0

ANOVA

Source of Variation	*SS*	*df*	*MS*	*F*	*P-value*	*F crit*
Between Groups	0.016714	1	0.016714	0.12786	0.754871	18.51282
Within Groups	0.261444	2	0.130722			
Total	0.278158	3				

East 1-wk vs West Old

SUMMARY

Groups	*Count*	*Sum*	*Average*	*Variance*
Column 1	2	2.169331	1.084665	0.261444
Column 2	2	2.933112	1.466556	0

ANOVA

Source of Variation	*SS*	*df*	*MS*	*F*	*P-value*	*F crit*
Between Groups	0.14584	1	0.14584	1.115652	0.401602	18.51282
Within Groups	0.261444	2	0.130722			
Total	0.407285	3				

East vs West Old

SUMMARY

Groups	*Count*	*Sum*	*Average*	*Variance*
Column 1	2	2.427897	1.213949	1.62E-13
Column 2	2	2.933113	1.466556	6.24E-13

ANOVA

Source of Variation	*SS*	*df*	*MS*	*F*	*P-value*	*F crit*
Between Groups	0.063811	1	0.063811	1.62E+11	6.16E-12	18.51282
Within Groups	7.86E-13	2	3.93E-13			
Total	0.063811	3				

East vs West Bottom

SUMMARY

Groups	*Count*	*Sum*	*Average*	*Variance*
Column 1	2	9.995774	4.997887	0.094438

Column 2	2	8.496962	4.248481	0

ANOVA

Source of Variation	*SS*	*df*	*MS*	*F*	*P-value*	*F crit*
Between Groups	0.56161	1	0.56161	11.89371	0.07477	18.51282
Within Groups	0.094438	2	0.047219			
Total	0.656048	3				

East Bot vs West 1-week

SUMMARY

Groups	*Count*	*Sum*	*Average*	*Variance*
Column 1	2	9.995774	4.997887	0.094438
Column 2	2	8.096405	4.048202	0.006502

ANOVA

Source of Variation	*SS*	*df*	*MS*	*F*	*P-value*	*F crit*
Between Groups	0.901901	1	0.901901	17.87005	0.051661	18.51282
Within Groups	0.10094	2	0.05047			
Total	1.002841	3				

East vs West 1-wk

SUMMARY

Groups	*Count*	*Sum*	*Average*	*Variance*
Column 1	2	8.096405	4.048202	0.006502
Column 2	2	2.169331	1.084665	0.261444

ANOVA

Source of Variation	*SS*	*df*	*MS*	*F*	*P-value*	*F crit*
Between Groups	8.782551	1	8.782551	65.55461	0.014914	18.51282
Within Groups	0.267946	2	0.133973			
Total	9.050497	3				

Data, Calculations, and ANOVA for Figure 12

Table 13. Calculation of TS, Ash, and VS weight and percent used in Figure 12

Sample	Tin #	Tin (g)	Tin+Wet (g)	Tin+Dry (g)	Tin+Ash (g)	Wet (g)	TS (g)	Ash (g)	VS (g)	TS (%)	Ash (%)	VS (%)
Trickling Filter (Stepped)	1	2.06	9.02	2.32	2.13	6.96	0.25	0.07	0.19	3.65	25.80	74.20
"	2	2.02	9.34	2.31	2.08	7.32	0.28	0.06	0.23	3.89	19.77	80.23
Trickling Filter (Filamentous)	3	2.03	6.81	2.32	2.10	4.78	0.28	0.07	0.22	5.94	23.50	76.50
"	4	2.03	4.09	2.18	2.09	2.06	0.15	0.06	0.09	7.25	39.34	60.66
Trickling Filter (Film)	5	2.07	6.06	2.22	2.08	4.00	0.15	0.01	0.14	3.85	6.83	93.17
"	6	2.04	5.74	2.31	2.12	3.70	0.27	0.08	0.19	7.19	29.93	70.07
Sludge	7	2.08	9.58	2.29	spilled	7.50	0.21	spilled	spilled	2.80	spilled	spilled
"	8	2.16	7.41	2.30	2.20	5.26	0.15	0.04	0.10	2.79	29.99	70.01
"	9	2.03	3.89	2.09	2.05	1.86	0.05	0.02	0.04	2.79	30.89	69.11
SE Poly (Bottom)	10	2.07	3.73	2.48	2.27	1.66	0.41	0.20	0.21	24.79	49.60	50.40
"	11	2.05	3.12	2.31	2.18	1.07	0.27	0.13	0.13	24.81	49.91	50.09
SE Poly (1 wk - productivity)	12	2.11	5.54	2.44	2.24	3.43	0.33	0.13	0.20	9.58	40.38	59.62
SE Poly (1 wk)	13	2.08	5.91	2.38	2.21	3.83	0.30	0.13	0.17	7.77	43.83	56.17
SE Poly (Old)	14	2.11	3.29	2.23	2.17	1.18	0.12	0.06	0.06	10.56	51.73	48.27
"	15	2.06	3.16	2.19	2.13	1.10	0.12	0.06	0.06	11.04	51.90	48.10
SW Poly (Bottom)	16	2.08	3.61	2.48	2.36	1.53	0.40	0.28	0.12	25.92	69.82	30.18
"	17	2.07	3.16	2.35	2.25	1.09	0.28	0.18	0.10	25.96	64.30	35.70

Continued…

Table 13 continued…

Sample	Tin #	Tin (g)	Tin+Wet (g)	Tin+Dry (g)	Tin+Ash (g)	Wet (g)	TS (g)	Ash (g)	VS (g)	TS (%)	Ash (%)	VS (%)
SW Poly (1 wk - Productivity)	18	2.11	10.09	3.24	2.74	7.98	1.13	0.63	0.50	14.19	55.95	44.05
" (add together previous)	19	2.08	11.66	3.45	2.85	9.58	1.38	0.77	0.60	14.35	56.14	43.86
SW Poly (Top, Old)	20	2.04	4.08	2.25	2.15	2.04	0.22	0.11	0.11	10.71	51.05	48.95
"	21	2.03	3.74	2.22	2.13	1.71	0.18	0.09	0.09	10.74	51.42	48.58
SW Poly (1 wk)	22	2.06	3.05	2.22	2.15	0.99	0.17	0.09	0.07	16.72	55.26	44.74

Table 14. Calculation of TS, Ash, and VS average and standard deviation from data in Table 13 for use in Figure 12

	Wet (g)	TS (g)	Ash (g)	VS (g)	TS (%)	Ash (%)	VS (%)
Trickling Filter Average	4.80	0.23	0.06	0.18	5.29	24.20	75.80
Trickling Filter SD	2.02	0.06	0.02	0.05	1.71	10.83	10.83
Trickling Filter Coeff of Var	42.02	27.34	42.41	29.13	32.28	44.76	14.29
Sludge Average	4.87	0.14	0.03	0.07	2.79	30.44	69.56
Sludge SD	2.84	0.08	0.02	0.05	0.01	0.63	0.63
Sludge Coeff of Var	58.37	58.50	66.00	68.31	0.18	2.08	0.91
SE Poly (Bottom) Average	1.37	0.34	0.17	0.17	24.80	49.75	50.25
SE Poly (Bottom) SD	0.42	0.10	0.05	0.05	0.02	0.22	0.22
SE Poly (Bottom) Coeff of var	30.73	30.67	30.25	31.08	0.06	0.44	0.43
SE Poly (1 wk) Average	3.63	0.31	0.13	0.18	8.67	42.11	57.89
SE Poly (1 wk) SD	0.28	0.02	0.00	0.02	1.28	2.44	2.44
SE Poly (1 wk) Coeff of Var	7.73	7.07	1.29	11.26	14.76	5.78	4.21
SE Poly (Old) Average	1.14	0.12	0.06	0.06	10.80	51.81	48.19
SE Poly (Old) SD	0.06	0.00	0.00	0.00	0.34	0.12	0.12
SE Poly (Old) Coeff of Var	5.04	1.90	1.67	2.15	3.14	0.23	0.25
SW Poly (Bottom) Average	1.31	0.34	0.23	0.11	25.94	67.06	32.94
SW Poly (Bottom) SD	0.31	0.08	0.07	0.01	0.03	3.91	3.91
SW Poly (Bottom) Coeff of var	23.68	23.57	29.19	11.88	0.12	5.82	11.86
SW Poly (1 wk) Average	6.19	0.89	0.50	0.39	15.09	55.78	44.22
SW Poly (1 wk) SD	4.57	0.64	0.36	0.28	1.42	0.46	0.46
SW Poly (1 wk) Coeff of Var	73.82	71.75	72.01	71.42	9.39	0.83	1.05
SW Poly (Top, Old) Average	1.87	0.20	0.10	0.10	10.73	51.24	48.76
SW Poly (Top, Old) SD	0.24	0.03	0.01	0.01	0.02	0.26	0.26
SW Poly (Top, Old) Coeff of Var	12.71	12.52	12.02	13.05	0.18	0.51	0.53

Table 15. ANOVA: Single factor for statistical significance between TS, Ash, and VS between CVWRF RABR microalgae biofilm layers. data from Table 13 was analyzed using Microsoft Excel Data Analysis. A p-value <0.05 is considered significantly different. Significantly different p-values are highlighted yellow while insignificant differences are highlighted red.

SE Poly TS(%) all layers

SUMMARY

Groups	*Count*	*Sum*	*Average*	*Variance*
Column 1	2	49.59835	24.79917	0.000256
Column 2	2	17.34734	8.673671	1.639451
Column 3	2	21.59905	10.79953	0.114941

ANOVA

Source of Variation	*SS*	*df*	*MS*	*F*	*P-value*	*F crit*
Between Groups	307.0275	2	153.5138	262.4694	0.000428	9.552094
Within Groups	1.754648	3	0.584883			
Total	308.7822	5				

SE Poly TS(%) Bottom vs 1-wk

SUMMARY

Groups	*Count*	*Sum*	*Average*	*Variance*
Column 1	2	49.59835	24.79917	0.000256
Column 2	2	17.34734	8.673671	1.639451

ANOVA

Source of Variation	*SS*	*df*	*MS*	*F*	*P-value*	*F crit*
Between Groups	260.0319	1	260.0319	317.1688	0.003138	18.51282
Within Groups	1.639706	2	0.819853			
Total	261.6716	3				

SE Poly TS(%) 1-wk vs Old

SUMMARY

Groups	*Count*	*Sum*	*Average*	*Variance*
Column 1	2	17.34734	8.673671	1.639451
Column 2	2	21.59905	10.79953	0.114941

ANOVA

Source of Variation	*SS*	*df*	*MS*	*F*	*P-value*	*F crit*
Between Groups	4.519262	1	4.519262	5.151941	0.151262	18.51282
Within Groups	1.754392	2	0.877196			
Total	6.273654	3				

SE Poly TS(%) Bottom vs Old

SUMMARY

Groups	*Count*	*Sum*	*Average*	*Variance*
Column 1	2	49.59835	24.79917	0.000256
Column 2	2	21.59905	10.79953	0.114941

ANOVA

Source of Variation	*SS*	*df*	*MS*	*F*	*P-value*	*F crit*
Between Groups	195.9902	1	195.9902	3402.701	0.000294	18.51282
Within Groups	0.115197	2	0.057598			
Total	196.1053	3				

SE Poly Ash(%) all layers

SUMMARY

Groups	*Count*	*Sum*	*Average*	*Variance*
Column 1	2	99.50511	49.75256	0.046903
Column 2	2	84.21123	42.10561	5.931734
Column 3	2	103.6246	51.8123	0.014583

ANOVA

Source of Variation	*SS*	*df*	*MS*	*F*	*P-value*	*F crit*
Between Groups	104.6253	2	52.31266	26.18592	0.012611	9.552094
Within Groups	5.99322	3	1.99774			
Total	110.6185	5				

SE Poly Ash(%) Bottom vs 1-wk

SUMMARY

Groups	*Count*	*Sum*	*Average*	*Variance*
Column 1	2	99.50511	49.75256	0.046903
Column 2	2	84.21123	42.10561	5.931734

ANOVA

Source of Variation	*SS*	*df*	*MS*	*F*	*P-value*	*F crit*
Between Groups	58.47573	1	58.47573	19.56156	0.047507	18.51282
Within Groups	5.978637	2	2.989319			
Total	64.45437	3				

SE Poly Ash(%) 1-wk vs Old

SUMMARY

Groups	*Count*	*Sum*	*Average*	*Variance*
Column 1	2	103.6246	51.8123	0.014583
Column 2	2	84.21123	42.10561	5.931734

ANOVA

Source of Variation	*SS*	*df*	*MS*	*F*	*P-value*	*F crit*
Between Groups	94.21972	1	94.21972	31.69011	0.030136	18.51282
Within Groups	5.946317	2	2.973159			
Total	100.166	3				

SE Poly Ash(%) Bottom vs Old

SUMMARY

Groups	*Count*	*Sum*	*Average*	*Variance*
Column 1	2	99.50511	49.75256	0.046903
Column 2	2	103.6246	51.8123	0.014583

ANOVA

Source of Variation	*SS*	*df*	*MS*	*F*	*P-value*	*F crit*
Between Groups	4.242537	1	4.242537	137.9988	0.007169	18.51282
Within Groups	0.061487	2	0.030743			
Total	4.304024	3				

SW Poly TS(%) all layers

SUMMARY

Groups	*Count*	*Sum*	*Average*	*Variance*
Column 1	2	51.87726	25.93863	0.000895
Column 2	2	28.53713	14.26856	0.013152
Column 3	2	21.45565	10.72783	0.000386

ANOVA

Source of Variation	*SS*	*df*	*MS*	*F*	*P-value*	*F crit*
Between Groups	253.3971	2	126.6986	26334.82	4.3E-07	9.552094
Within Groups	0.014433	3	0.004811			
Total	253.4116	5				

SW Poly TS(%) Bottom Vs 1-wk

SUMMARY

Groups	*Count*	*Sum*	*Average*	*Variance*
Column 1	2	51.87726	25.93863	0.000895
Column 2	2	28.53713	14.26856	0.013152

ANOVA

Source of Variation	*SS*	*df*	*MS*	*F*	*P-value*	*F crit*
Between Groups	136.1904	1	136.1904	19390.29	5.16E-05	18.51282
Within Groups	0.014047	2	0.007024			
Total	136.2044	3				

SW Poly TS(%) 1-wk vs Old

SUMMARY

Groups	*Count*	*Sum*	*Average*	*Variance*
Column 1	2	21.45565	10.72783	0.000386
Column 2	2	28.53713	14.26856	0.013152

ANOVA

Source of Variation	*SS*	*df*	*MS*	*F*	*P-value*	*F crit*
Between Groups	12.53683	1	12.53683	1852.045	0.00054	18.51282
Within Groups	0.013538	2	0.006769			
Total	12.55036	3				

SW Poly TS(%) Bottom vs Old

Groups	*Count*	*Sum*	*Average*	*Variance*
Column 1	2	51.87726	25.93863	0.000895
Column 2	2	21.45565	10.72783	0.000386

ANOVA

Source of Variation	*SS*	*df*	*MS*	*F*	*P-value*	*F crit*
Between Groups	231.3685	1	231.3685	361299	2.77E-06	18.51282

Within Groups	0.001281	2	0.00064
Total	231.3698	3	

SW Poly Ash(%) all layers

SUMMARY

Groups	*Count*	*Sum*	*Average*	*Variance*
Column 1	2	134.1147	67.05734	15.25253
Column 2	2	112.0914	56.04569	0.017968
Column 3	2	102.4704	51.2352	0.067721

ANOVA

Source of Variation	*SS*	*df*	*MS*	*F*	*P-value*	*F crit*
Between Groups	263.1583	2	131.5792	25.73555	0.012925	9.552094
Within Groups	15.33822	3	5.11274			
Total	278.4965	5				

SW Poly Ash(%) Bottom vs 1-wk

SUMMARY

Groups	*Count*	*Sum*	*Average*	*Variance*
Column 1	2	134.1147	67.05734	15.25253
Column 2	2	112.0914	56.04569	0.017968

ANOVA

Source of Variation	*SS*	*df*	*MS*	*F*	*P-value*	*F crit*
Between Groups	121.2564	1	121.2564	15.88114	0.057583	18.51282
Within Groups	15.2705	2	7.63525			
Total	136.5269	3				

SW Poly Ash(%) 1-wk vs Old

SUMMARY

Groups	*Count*	*Sum*	*Average*	*Variance*
Column 1	2	102.4704	51.2352	0.067721
Column 2	2	112.0914	56.04569	0.017968

ANOVA

Source of Variation	*SS*	*df*	*MS*	*F*	*P-value*	*F crit*
Between Groups	23.14084	1	23.14084	540.1081	0.001846	18.51282
Within Groups	0.08569	2	0.042845			
Total	23.22653	3				

SW Poly Ash(%) Bottom vs Old

SUMMARY

Groups	*Count*	*Sum*	*Average*	*Variance*
Column 1	2	134.1147	67.05734	15.25253
Column 2	2	102.4704	51.2352	0.067721

ANOVA

Source of Variation	*SS*	*df*	*MS*	*F*	*P-value*	*F crit*
Between Groups	250.3402	1	250.3402	32.68095	0.029262	18.51282
Within Groups	15.32025	2	7.660126			
Total	265.6605	3				

TS(%) of SE vs SW poly Bottom

SUMMARY

Groups	*Count*	*Sum*	*Average*	*Variance*

Column 1	2	49.59835	24.79917	0.000256
Column 2	2	51.87726	25.93863	0.000895

ANOVA

Source of Variation	*SS*	*df*	*MS*	*F*	*P-value*	*F crit*
Between Groups	1.298354	1	1.298354	2256.951	0.000443	18.51282
Within Groups	0.001151	2	0.000575			
Total	1.299505	3				

Ash(%) of SE vs SW poly Bottom

SUMMARY

Groups	*Count*	*Sum*	*Average*	*Variance*
Column 1	2	99.50511	49.75256	0.046903
Column 2	2	134.1147	67.05734	15.25253

ANOVA

Source of Variation	*SS*	*df*	*MS*	*F*	*P-value*	*F crit*
Between Groups	299.4557	1	299.4557	39.14598	0.024606	18.51282
Within Groups	15.29943	2	7.649717			
Total	314.7551	3				

TS(%) of SE vs SW poly 1 wk

SUMMARY

Groups	*Count*	*Sum*	*Average*	*Variance*
Column 1	2	17.34734	8.673671	1.639451
Column 2	2	28.53713	14.26856	0.013152

ANOVA

Source of Variation	*SS*	*df*	*MS*	*F*	*P-value*	*F crit*
Between Groups	31.30284	1	31.30284	37.88307	0.025396	18.51282
Within Groups	1.652603	2	0.826302			

Total	32.95544	3				

Ash(%) of SE vs SW poly 1 wk

SUMMARY

Groups	*Count*	*Sum*	*Average*	*Variance*
Column 1	2	84.21123	42.10561	5.931734
Column 2	2	112.0914	56.04569	0.017968

ANOVA

Source of Variation	*SS*	*df*	*MS*	*F*	*P-value*	*F crit*
Between Groups	194.3258	1	194.3258	65.32288	0.014966	18.51282
Within Groups	5.949702	2	2.974851			
Total	200.2755	3				

TS(%) of SE vs SW poly Old

SUMMARY

Groups	*Count*	*Sum*	*Average*	*Variance*
Column 1	2	21.59905	10.79953	0.114941
Column 2	2	21.45565	10.72783	0.000386

ANOVA

Source of Variation	*SS*	*df*	*MS*	*F*	*P-value*	*F crit*
Between Groups	0.005141	1	0.005141	0.089152	0.793423	18.51282
Within Groups	0.115327	2	0.057664			
Total	0.120468	3				

Ash(%) of SE vs SW poly Old

SUMMARY

Groups	*Count*	*Sum*	*Average*	*Variance*

Column 1	2	103.6246	51.8123	0.014583
Column 2	2	102.4704	51.2352	0.067721

ANOVA

Source of Variation	*SS*	*df*	*MS*	*F*	*P-value*	*F crit*
Between Groups	0.333042	1	0.333042	8.092892	0.104544	18.51282
Within Groups	0.082305	2	0.041152			
Total	0.415346	3				

TS% E Bot vs W 1 wk

SUMMARY

Groups	*Count*	*Sum*	*Average*	*Variance*
Column 1	2	49.59835	24.79917	0.000256
Column 2	2	28.53713	14.26856	0.013152

ANOVA

Source of Variation	*SS*	*df*	*MS*	*F*	*P-value*	*F crit*
Between Groups	110.8937	1	110.8937	16541.26	6.04E-05	18.51282
Within Groups	0.013408	2	0.006704			
Total	110.9072	3				

TS% E Bot vs W Old

SUMMARY

Groups	*Count*	*Sum*	*Average*	*Variance*
Column 1	2	49.59835	24.79917	0.000256
Column 2	2	21.45565	10.72783	0.000386

ANOVA

Source of Variation	*SS*	*df*	*MS*	*F*	*P-value*	*F crit*

Between Groups	198.0028	1	198.0028	617196.6	1.62E-06	18.51282
Within Groups	0.000642	2	0.000321			
Total	198.0035	3				

TS% E 1wk vs W Old

SUMMARY

Groups	*Count*	*Sum*	*Average*	*Variance*
Column 1	2	17.34734	8.673671	1.639451
Column 2	2	21.45565	10.72783	0.000386

ANOVA

Source of Variation	*SS*	*df*	*MS*	*F*	*P-value*	*F crit*
Between Groups	4.219557	1	4.219557	5.146313	0.151392	18.51282
Within Groups	1.639837	2	0.819918			
Total	5.859394	3				

TS% E 1wk vs W Bot

SUMMARY

Groups	*Count*	*Sum*	*Average*	*Variance*
Column 1	2	17.34734	8.673671	1.639451
Column 2	2	51.87726	25.93863	0.000895

ANOVA

Source of Variation	*SS*	*df*	*MS*	*F*	*P-value*	*F crit*
Between Groups	298.0788	1	298.0788	363.4341	0.00274	18.51282
Within Groups	1.640346	2	0.820173			
Total	299.7191	3				

TS% E Old vs W Bot

SUMMARY

Groups	*Count*	*Sum*	*Average*	*Variance*
Column 1	2	21.59905	10.79953	0.114941
Column 2	2	51.87726	25.93863	0.000895

ANOVA

Source of Variation	*SS*	*df*	*MS*	*F*	*P-value*	*F crit*
Between Groups	229.1924	1	229.1924	3957.19	0.000253	18.51282
Within Groups	0.115836	2	0.057918			
Total	229.3082	3				

TS% E Old vs W 1wk

SUMMARY

Groups	*Count*	*Sum*	*Average*	*Variance*
Column 1	2	21.59905	10.79953	0.114941
Column 2	2	28.53713	14.26856	0.013152

ANOVA

Source of Variation	*SS*	*df*	*MS*	*F*	*P-value*	*F crit*
Between Groups	12.03423	1	12.03423	187.8975	0.00528	18.51282
Within Groups	0.128094	2	0.064047			
Total	12.16232	3				

Ash % E Bot vs W 1wk

SUMMARY

Groups	*Count*	*Sum*	*Average*	*Variance*
Column 1	2	99.5051	49.7525	0.04690 3
Column 2	2	112.091 4	56.0456 9	0.01796 8

ANOVA

Source of Variation	*SS*	*df*	*MS*	*F*	*P-value*	*F crit*
Between Groups	39.60358	1	39.60358	1220.985	0.000818	18.51282
Within Groups	0.064872	2	0.032436			
Total	39.66845	3				

Ash % E Bot vs W Old

SUMMARY

Groups	*Count*	*Sum*	*Average*	*Variance*
Column 1	2	99.50511	49.75256	0.046903
Column 2	2	102.4704	51.2352	0.067721

ANOVA

Source of Variation	*SS*	*df*	*MS*	*F*	*P-value*	*F crit*
Between Groups	2.198235	1	2.198235	38.35532	0.025095	18.51282
Within Groups	0.114625	2	0.057312			
Total	2.312859	3				

Ash % E 1wk vs W old

SUMMARY

Groups	*Count*	*Sum*	*Average*	*Variance*
Column 1	2	84.21123	42.10561	5.931734
Column 2	2	102.4704	51.2352	0.067721

ANOVA

Source of Variation	*SS*	*df*	*MS*	*F*	*P-value*	*F crit*
Between Groups	83.34936	1	83.34936	27.78564	0.034157	18.51282
Within Groups	5.999455	2	2.999728			

Total	89.34881	3				

Ash % E 1wk vs W bot

SUMMARY

Groups	*Count*	*Sum*	*Average*	*Variance*
Column 1	2	84.21123	42.10561	5.931734
Column 2	2	134.1147	67.05734	15.25253

ANOVA

Source of Variation	*SS*	*df*	*MS*	*F*	*P-value*	*F crit*
Between Groups	622.5888	1	622.5888	58.77842	0.016591	18.51282
Within Groups	21.18427	2	10.59213			
Total	643.7731	3				

Ash % E Old vs W bot

SUMMARY

Groups	*Count*	*Sum*	*Average*	*Variance*
Column 1	2	103.6246	51.8123	0.014583
Column 2	2	134.1147	67.05734	15.25253

ANOVA

Source of Variation	*SS*	*df*	*MS*	*F*	*P-value*	*F crit*
Between Groups	232.4114	1	232.4114	30.44602	0.031311	18.51282
Within Groups	15.26711	2	7.633557			
Total	247.6785	3				

Ash % E Old vs W 1wk

SUMMARY

Groups	*Count*	*Sum*	*Average*	*Variance*
Column 1	2	103.6246	51.8123	0.014583

Column 2	2	112.0914	56.04569	0.017968

ANOVA

Source of Variation	*SS*	*df*	*MS*	*F*	*P-value*	*F crit*
Between Groups	17.92164	1	17.92164	1101.126	0.000907	18.51282
Within Groups	0.032551	2	0.016276			
Total	17.95419	3				

Data and Calculations for Figure 13

Table 16. Data from ICP-MS for Mg, Ca, and P content of CVWRF RABR microalgae biofilm layers

		24 Mg [He]	31 P [He]	44 Ca [He]
Top Limit		**100**	**10**	**100**
MRL	**3/19/2019**	**0.03**	**0.10**	**0.03**
MDL	**3/19/2019**	0.002	0.037	0.007
Sample Name	Dilution	Conc. [mg/l]	Conc. [mg/l]	Conc. [mg/l]
23 Trickling filter	Combined	46.68	187.66	320.98
24 Sludge	Combined	16.34	80.34	157.43
25 SE Poly bot	Combined	591.25	724.17	71.14
26 SE Poly 1 wk 1	Combined	113.64	172.03	56.43
27 SE Poly old	Combined	99.29	94.39	47.29
28 SW Poly Bot	Combined	706.30	997.00	121.91
29 SW Poly 1 wk	Combined	1094.72	1643.66	260.00
30 SW Poly old	Combined	140.39	215.07	70.66

Table 17. Calculations for Mg, P, and Ca content of Ash and TS. The columns highlighted blue are data from Table 14.

	24 Mg [He]	31 P [He]	44 Ca [He]	Ash (mg/L)	mg / mg Ash	mg P / mg Ash	mg Ca / mg Ash	mol Mg / mg Ash	mol P / mg Ash	mol Ca / mg Ash	mg Ash / mg TS	mg / mg TS	mg P / mg TS	mg Ca / mg TS
Sample Name	Conc. [mg/l]	Conc. [mg/l]	Conc. [mg/l]											
23 Trickling filter	4.7E+01	1.9E+02	3.2E+02	3.2E+03	1.4E-02	5.8E-02	9.9E-02	5.9E-07	1.9E-06	2.5E-06	2.4E-01	3.5E-03	1.4E-02	2.4E-02
24 Sludge	1.6E+01	8.0E+01	1.6E+02	9.9E+02	1.6E-02	8.1E-02	1.6E-01	6.8E-07	2.6E-06	3.9E-06	2.2E-01	3.6E-03	1.8E-02	3.5E-02
25 SE Poly bot	5.9E+02	7.2E+02	7.1E+01	3.3E+03	1.8E-01	2.2E-01	2.2E-02	7.4E-06	7.1E-06	5.4E-07	5.0E-01	8.9E-02	1.1E-01	1.1E-02
26 SE Poly 1 wk 1	1.1E+02	1.7E+02	5.6E+01	2.5E+03	4.5E-02	6.8E-02	2.2E-02	1.9E-06	2.2E-06	5.6E-07	4.2E-01	1.9E-02	2.9E-02	9.4E-03
27 SE Poly old	9.9E+01	9.4E+01	4.7E+01	1.2E+03	8.1E-02	7.7E-02	3.8E-02	3.3E-06	2.5E-06	9.6E-07	5.2E-01	4.2E-02	4.0E-02	2.0E-02
28 SW Poly Bot	7.1E+02	1.0E+03	1.2E+02	4.4E+03	1.6E-01	2.3E-01	2.8E-02	6.7E-06	7.4E-06	7.0E-07	6.8E-01	1.1E-01	1.5E-01	1.9E-02
29 SW Poly 1 wk	1.1E+03	1.6E+03	2.6E+02	7.1E+03	1.5E-01	2.3E-01	3.7E-02	6.4E-06	7.5E-06	9.2E-07	5.6E-01	8.7E-02	1.3E-01	2.1E-02
30 SW Poly old	1.4E+02	2.2E+02	7.1E+01	2.0E+03	7.0E-02	1.1E-01	3.5E-02	2.9E-06	3.4E-06	8.8E-07	5.1E-01	3.6E-02	5.5E-02	1.8E-02

Table 18. Mg and Ca in biofilm ash normalized per mole P using data from Table 17. The data in the last three columns was graphed in Figure 6.

	mol Mg / mg Ash	mol P / mg Ash	mol Ca / mg Ash	mol NH3 / mg Ash	mol Mg / mol P	mol Ca / mol P	mol NH3 / mol P
23 Trickling filter	5.9E-07	1.9E-06	2.5E-06	2.7E-08	3.2E-01	1.3E+00	1.5E-02
24 Sludge	6.8E-07	2.6E-06	3.9E-06	1.8E-07	2.6E-01	1.5E+00	6.8E-02
25 SE Poly bot	7.4E-06	7.1E-06	5.4E-07	4.1E-07	1.0E+00	7.6E-02	5.8E-02
26 SE Poly 1 wk 1	1.9E-06	2.2E-06	5.6E-07	1.1E-07	8.4E-01	2.5E-01	4.8E-02
27 SE Poly old	3.3E-06	2.5E-06	9.6E-07	9.5E-08	1.3E+00	3.9E-01	3.9E-02
28 SW Poly Bot	6.7E-06	7.4E-06	7.0E-07	2.6E-07	9.0E-01	9.4E-02	3.5E-02
29 SW Poly 1 wk	6.4E-06	7.5E-06	9.2E-07	2.9E-07	8.5E-01	1.2E-01	3.9E-02
30 SW Poly old	2.9E-06	3.4E-06	8.8E-07	1.2E-07	8.3E-01	2.5E-01	3.4E-02

Chapter 2 Appendix

Data for Figure 15

Table 19. ICP-MS precipitation test data for Mg, Ca, and P content of dissolved precipitates. Mg and Ca molar concentration was normalized to P for use in Figure 15.

	Mg	Ca	P	Mg	Ca	P	Mg/P	Ca/P
pH	mg/L	mg/L	mg/L	mol/L	mol/L	mol/L	molar	molar
7.9	0.52	2.61	1.16	2.14E-05	6.51E-05	3.75E-05	5.70E-01	1.74E+00
8	0.92	4.14	1.82	3.78E-05	1.03E-04	5.88E-05	6.43E-01	1.76E+00
8.1	1.01	4.06	1.80	4.16E-05	1.01E-04	5.82E-05	7.15E-01	1.74E+00
8.2	1.14	4.40	2.20	4.71E-05	1.10E-04	7.11E-05	6.62E-01	1.55E+00
8.3	3.42	5.78	5.30	1.41E-04	1.44E-04	1.71E-04	8.22E-01	8.42E-01

Chapter 3 Appendix

Data and Calculations for Figure 17

Table 20. Temperature and pH data for tank water and microalgae biofilm of APP RABRs. Only data between July 10 and August 29 were included in Figure 17 because suspended growth significantly increased pH prior to July 7. White HDPE paneling was added to cover RABR water and reflect sunlight on July 7. The "Day" column represents the number of days since the last water change.

Date (2019)	Sample	Day	pH	mV	Temp (C)
7-Mar	RABR 1		8.15	-61	26
			8.18	-65	26
			8.13	-63	26
	RABR 2		8.14	-63	26
			8.08	-60	26
			8.1	-61	26
24-Mar	RABR 1				16.7
	RABR 2				15.8
9-Apr	RABR 1		7.89	-57	17.7
			7.75	-56	
			7.77	-58	
	RABR 2		8.74		17.4
			8.75		
			8.74	-110	
16-Apr	RABR 1		6.54		20.1
			6.63		
			6.62		
	RABR 2		8.69		
			8.78	-116	19.6
			8.77	-115	

Continued…

Table 20 Continued…

Date (2019)	Sample	Day	pH	mV	Temp (C)
22-May	RABR 1 Water		9.88	-157	18.1
			9.89	-157	18.2
			9.9	-158	18.2
	RABR 1 Biofilm		9.5	-136	19.6
			9.7	-148	20.8
			9.26	-125	23.7
	RABR 2 Water		9.97	-162	18.6
			9.97	-162	18.6
			9.97	-162	18.6
21-Jun	RABR 1 Water		9.42	-129	14.1
			9.44	-0.1	14.1
			9.46	-131	14.1
	RABR 1 Biofilm		9.17	-115	12.4
			9.33	-122	9.9
			9.21	-116	10
	RABR 2 Water		9.07	-110	14.1
			9.07	-110	14
			9.08	-110	14.1
	RABR 2 Biofilm		8.94	-101	10.4
			8.95	-102	9.9
			8.95	-102	9.4
1-Jul	RABR 1 Water		9.81	-154	24.8
			9.81	-155	24.8
			9.83	-156	24.8
	RABR 2 Water		9.83	-156	25.7
			9.85	-158	25.7
			9.86	-158	25.7
	RABR 1 Biofilm		9.59	-144	27
			9.31	-125	26.2
			9.14	-118	27.6
	RABR 2 Biofilm		9.29	-127	27.6
			9.27	-126	27.9
			9.18	-119	23.8

Continued…

Table 20 Continued…

Date (2019)	Sample	Day	pH	mV	Temp (C)
2-Jul	RABR 1 water	0	8.17	-62	25.8
			8.18	-63	25.8
			8.17	-63	25.8
	RABR 2 Water		8.14	-61	26.7
			8.15	-61	26.6
			8.15	-62	26.6
3-Jul	RABR 1 Water	1	8.45	-77	21.1
			8.48	-79	21.5
			8.48	-78	21.6
	RABR 2 Water		8.49	-79	22.4
			8.48	-79	22.7
			8.48	-79	22.7
10-Jul	RABR 1 Water	9	8.49	-80	20.5
			8.5	-81	20.8
			8.51	-81	21
	RABR 2 Water		8.49	-81	22.7
			8.5	-81	23
			8.49	-81	23
	RABR 1 Biofilm		8.44	-79	25.9
			8.41	-76	23.1
			8.47	-79	22.7
	RABR 2 Biofilm		8.47	-80	25.3
			8.46	-79	23.5
			8.44	-78	24.5
17-Jul	RABR 1 Water	16	7.86	-44	23.2
			7.86	-44	23.3
			7.87	-44	23.5
	RABR 2 Water		7.84	-43	22.6
			7.85	-43	22.7
			7.85	-43	22.8

Continued…

Table 20 Continued…

Date (2019)	Sample	Day	pH	mV	Temp (C)
	RABR 1 Biofilm		8.22	-65	26.5
			8.22	-64	21.3
			8.06	-55	20.1
	RABR 2 Biofilm		8.05	-54	21.5
			8.16	-60	20.6
			8.15	-60	21.6
19-Jul	RABR 1 Water	18	8.36	-74	21.3
			8.41	-77	21.5
			8.43	-78	21.6
	RABR 2 Water		8.17	-64	21.9
			8.24	-67	22
			8.28	-70	22
22-Jul	RABR 1 Water	21	8.4	-78	21.8
			8.42	-79	21.8
			8.43	-79	21.8
	RABR 2 Water		8.39	-77	22.8
			8.39	-77	22.9
			8.39	-77	22.9
	RABR 1 Biofilm		8.41	-79	25.1
			8.45	-81	23.7
			8.36	-76	23.6
	RABR 2 Biofilm		8.25	-71	28.6
			8.27	-71	25.2
			8.21	-69	29.5
Water changed					
24-Jul	RABR 1 Water	1	8.3	-73	24.6
			8.29	-73	24.6
			8.29	-73	24.6
	RABR 2 Water		8.28	-73	25.7
			8.27	-72	25.6
			8.27	-72	25.6
29-Jul	RABR 1 Water	6	7.99	-56	24.9
			7.99	-55	24.9
			7.99	-56	24.9

Continued…

Table 20 Continued…

Date (2019)	Sample	Day	pH	mV	Temp (C)
	RABR 2 Water		8.09	-60	23.9
			8.09	-61	24
			8.09	-60	24
1-Aug	RABR 1 Water	9	7.39	-24	18
			7.36	-22	18
			7.3	-22	18
	RABR 2 Water		7.64	-37	18.9
			7.66	-38	19
			7.66	-38	19
	RABR 1 Biofilm		7.38	-23	18.5
			7.26	-18	18.8
			7.23	-16	18.8
	RABR 2 Biofilm		7.67	-39	19.5
			7.67	-38	19.4
			7.78	-44	19.8
5-Aug	RABR 1 Water	13	7.06	-1	19.8
			7.09	-3	19.9
			7.09	-3	20
	RABR 2 Water		7.32	-15	20.6
			7.3	-14	20.7
			7.34	-16	20.8
	RABR 1 Biofilm		7.4	-20	23.6
			7.33	-16	23.7
			7.49	-25	23.7
	RABR 2 Biofilm		7.01	2	25.2
			7.63	-33	24.6
			7.82	-43	24.5
8-Aug	RABR 1 Water	16	7.56	-29	21.5
			7.58	-30	21.4
	RABR 2 Water		7.96	-50	20.4
			7.97	-51	20.6

Continued…

Table 20 Continued…

Date (2019)	Sample	Day	pH	mV	Temp (C)
	RABR 1 Biofilm		7.86	-45	20.1
			7.57	-29	20.1
			7.87	-45	19.8
	RABR 2 Biofilm		7.99	-52	19.6
			7.94	-49	20.1
			7.99	-52	20.3
Water Changed					
13-Aug	RABR 1 Water	0	7.95	-52	28.5
			7.97	-53	28.4
			8	-55	28.3
	RABR 2 Water		8.03	-56	27
			8.03	-56	26.9
			8.04	-57	26.8
	RABR 1 Biofilm		8.12	-61	25.4
			8.16	-64	25.4
			8.17	-64	25.4
	RABR 2 Biofilm		8.08	-59	27
			8.14	-62	25.7
			8.14	-62	25.5
14-Aug	R1 Water	1	8.38	-75	23.6
			8.37	-75	23
			8.37	-75	24.1
	R2 Water		8.34	-73	23.4
			8.35	-74	23.5
			8.35	-74	23.5
	R1 Biofilm		8.37	-75	23.5
			8.38	-75	24
			8.41	-77	23
	R2 Biofilm		8.18	-64	22.7
			8.39	-76	22.5
			8.37	-74	20.9

Continued…

Table 20 Continued…

Date (2019)	Sample	Day	pH	mV	Temp (C)
Water Refill					
26-Aug	R1 Water	0	7.86	-48	22.1
			7.88	-49	21.9
			7.89	-49	21.8
	R1 Carpet		7.92	-51	19.8
			7.95	-52	18.1
	R1 Polystyrene		8.01	-55	18.6
			8.01	-55	16.8
	R2 Water		8	-55	19.9
			8	-55	19.9
			8	-55	19.9
	R2 Carpet		8.08	-59	17.1
			8.13	-61	18.2
	R2 Poly		8.11	-61	18.2
			8.07	-58	17.7
27-Aug	R1 Water	1	7.9	-47	21.1
			7.91	-48	21.2
			7.91	-48	21.4
	R2 Water		8.02	-54	20.2
			8.03	-54	20.2
			8.03	-55	20.3
	R1 Biofilm poly		7.83	-44	24.4
			7.91	-48	23.7
			7.91	-48	23.5
	R2 Biofilm poly		8.03	-55	21.6
			8.04	-55	20.8
			8.08	-57	18.8

Table 21. Calculations for average and standard deviation of APP RABR water and biofilm pH using data from Table 20.

		Average pH				Standard Deviation			
Date (2019)	Day #	R1 Water	R1 Bio	R2 Water	R2 Bio	R1 Water	R1 Bio	R2 Water	R2 Bio
7-Mar	-	8.153333	-	8.106667	-	0.025166115	-	0.030551	-
9-Apr	-	7.803333	-	8.743333	-	0.075718778	-	0.005774	-
16-Apr	-	6.596667	-	8.746667	-	0.049328829	-	0.049329	
22-May	-	9.89	9.486667	9.97	-	0.01	0.220303	0	-
21-Jun	-	9.44	9.236667	9.073333	8.946667	0.02	0.083267	0.005774	0.005774
1-Jul	0	9.816667	9.346667	9.846667	9.246667	0.011547005	0.22723	0.015275	0.058595
2-Jul	1	8.173333	-	8.146667	-	0.005773503	-	0.005774	-
3-Jul	2	8.47	-	8.483333	-	0.017320508	-	0.005774	-
10-Jul	9	8.5	8.44	8.493333	8.456667	0.01	0.03	0.005774	0.015275
17-Jul	16	7.863333	8.166667	7.846667	8.12	0.005773503	0.092376	0.005774	0.060828
19-Jul	18	8.4	-	8.23	-	0.036055513	-	0.055678	
22-Jul	21	8.416667	8.406667	8.39	8.243333	0.015275252	0.045092	0	0.030551
24-Jul	1	8.293333	-	8.273333	-	0.005773503	-	0.005774	-
29-Jul	6	7.99	-	8.09	-	1.08779E-15	-	0	-
1-Aug	9	7.35	7.29	7.653333	7.706667	0.045825757	0.079373	0.011547	0.063509
5-Aug	13	7.08	7.406667	7.32	7.486667	0.017320508	0.080208	0.02	0.423596
8-Aug	16	7.57	7.766667	7.965	7.973333	0.014142136	0.170392	0.007071	0.028868
13-Aug	0	7.973333	8.15	8.033333	8.12	0.025166115	0.026458	0.005774	0.034641
14-Aug	1	8.373333	8.386667	8.346667	8.313333	0.005773503	0.020817	0.005774	0.115902
26-Aug	0	7.876667	7.9725	8	8.0975	0.015275252	0.045	0	0.027538
27-Aug	1	7.906667	7.883333	8.026667	8.05	0.005773503	0.046188	0.005774	0.026458
29-Aug	3	7.676667	7.65	7.906667	7.91	0.005773503	0.01	0.005774	0.017321

Data and Calculations for Figure 18

Table 22. Results from N, P, and Mg HACH kits on filtered APP RABR Water for use in Figure 14. Magnesium (Mg) as mg/L $CaCO_3$ was converted to mg/L by using the following formula: mg/L Mg = mg/L Mg as $CaCo_3$ * 50.04 / 12.5

Date (2019)	Sample	Day #	N (mg/L)	P (mg/L)	Mg (mg/L)	Total Hardness (mg/L CaCO3)	Ca Hardness (mg/L CaCO3)	Mg Hardness (mg/L CaCO3)
Water Changed								
24-Jul	RABR 1 Water	1	380	19.5	-	400	-	-
			390	19.9	82.4	420	400	20
			410	-	82.4	400	380	20
	RABR 2 Water		370	17.7	164.7	380	340	40
			390	17.1	0.0	360	360	0
			400	17.2	82.4	400	380	20
29-Jul	RABR 1 Water	6	150	31.3	741.3	480	300	180
			150	32	659.0	440	280	160
	RABR 2 Water		170	23.4	576.6	420	280	140
			140	25.2	576.6	420	280	140
1-Aug	RABR 1 Water	9	160	52.5	741.3	520	340	180
			180	51.2	659.0	500	340	160
	RABR 2 Water		150	33.7	659.0	460	300	160
			150	44.2	741.3	460	280	180

Continued…

Table 22 continued…

Date (2019)	Sample	Day #	N (mg/L)	P (mg/L)	Mg (mg/L)	Total Hardness (mg/L CaCO3)	Ca Hardness (mg/L CaCO3)	Mg Hardness (mg/L CaCO3)
5-Aug	RABR 1 Water	13	120	64.7	741.3	600	420	180
			160	66.9	576.6	540	400	140
	RABR 2 Water		120	39.9	741.3	500	320	180
			120	40.7	741.3	500	320	180
8-Aug	RABR 1 Water	16	130	46.6	659.0	620	460	160
			130	49	494.2	580	460	120
	RABR 2 Water		110	21.6	741.3	560	380	180
			120	23.9	576.6	520	380	140